Carbon nanotubes field effect transistors biosensors

Biosensores con transistores de efecto de campo basados en nanotubos de carbono

M.T. Martínez†*, Y.C. Tseng§, N. Ormategui,| I. Loinaz,| R. Eritja,¦ J.P. Salvador‡, M.P. Marco‡, J. Bokor§

†Instituto de Carboquímica. CSIC. Miguel Luesma 4. 50018 Zaragoza, España.

§Department of Electrical Engineering and Computer Sciences, University of California at Berkeley, Berkeley, California 94720-1770.

|CIDETEC Pº Miramón, 196 Parque Tecn. Miramón, 20009, San Sebastián, España.

¦Instituto de Quiímica Avanzada de Cataluña, CSIC, IRB Barcelona, CIBER-BBN, España.

‡Applied Molecular Receptors Group(AMRg), Chemical and Biomolecular Nanotechnology Department, IQAC-CSIC, Jorge Girona, 18-26, 08034 Barcelona, España.

** Corresponding autor: mtmartinez@icb.csic.es*

Abstract

Carbon nanotube transistor arrays (CNTFETs) were used as biosensors to detect DNA hybridization and to recognize two anabolic steroids, stanozolol (Stz) and methylboldenone (MB). Single strand DNA and antibodies specific for STz and MB were immobilized on the carbon nanotubes (CNTs) in situ in the device using two different approaches: direct noncovalent bonding of antibodies to the devices and covalently trough a polymer previously attached to the CNTFETs. A new approach to ensure specific adsorption of the biomolecules to the nanotubes was developed. The polymer poly (methylmethacrylate$_{0.8}$-co-poly (ethyleneglycol) methacrylate$_{0.8}$-co-N-succinimidyl methacrylate$_{0.1}$) was synthesized and bonded noncovalently to the nanotube. Aminated single-strand DNA or antibodies specific for Stz and MB were then attached covalently to the polymer. Statistically significant changes were observed in key transistor parameters for both DNA hybridization and steroids recognition. Regarding the detection mechanism, in addition to charge transfer, Schottky barrier, SB, modification, and scattering potential reported by other authors, an electron/hole trapping mechanism leading to hysteresis modification has been determined. The presence of polymer seems to hinder the modulation of the electrode-CNT contact.

Resumen

Matrices de transistores de efecto de campo basados en nanotubos de carbono (CNTFETs) fueron usados como biosensores para la detección de la hibridación de ADN y para el reconocimiento de dos esteroides anabolizantes, estazonolol (Stz) y metil-boldenona (MB). Secuencias simples de ADN y anticuerpos específicos para Stz y MB fueron inmovilizados sobre los nanotubos de carbono, (CNTs), in situ en los dispositivos usando dos estrategias diferentes; enlace directo no-covalente y enlace covalente a un polímero previamente fijado a los CNTFETs. Se ha desarrollado una nueva estrategia para asegurar la adsorción especifica de las biomoléculas a los CNTs. Se sintetizó el polímero poli (metilmetacrilato$_{0.8}$ -co-(polietilenglicol) metacrilato$_{0.8}$-co-N-succinimidil metacrilato$_{0.1}$) que fue enlazado no-covalentemente a los CNTs en el dispositivo. Posteriormente una secuencia simple de ADN o en su caso el correspondiente anticuerpo específico para Stz o MB fueron enlazados covalentemente al polímero. Se observaron cambios estadísticamente signiticativos en parámetros clave del transistor tanto para la hibridación de ADN como para el reconocimiento de los esteroides anabolizantes. Respecto al mecanismo de detección, además de transferencia de carga, modificación de la barrera de Schottky, SB, y dispersión de potencial publicados en la bibliografía, se ha detectado un mecanismo de atrapamiento de electrones y huecos que lleva a una modificación de la histéresis. La presencia del polímero parece impedir la modulación ejercida por los contactos electrodo-CNT.

1. Introduction

The broad applications of nanotechnology make it one of the most rapidly growing areas of research in contemporary science and medicine [1,2]. The unique chemical and optical properties of nanomaterials in terms of particle aggregation, photoemission, electrical and heat conductivity, and catalytic activity have paved the way for development of nanobioelectronic devices [3,4]. Micro- and nanofabrication has allowed the production of ultrasensitive, portable, and inexpensive biosensors. These devices generally rely on chemical or biological receptors that recognize a particular compound of interest and transfer this recognition event effectively [5].

The development and utilization of micro- and nanostructured materials, new semiconductor [6], quantum dots [7], plasmonic nanoparticles [8], nanowires [9] magnetic nanoparticles [10] and CNTs [11] have promoted extensive research activity in the field of biosensing, taking advantage of the many novel phenomena that occur at nanoscale.

Recently, one-dimensional nanostructures, such as carbon nanotubes and semiconductor nanowires, have been successfully demonstrated to be sensitive biological sensors [12]. CNTs show unique features that are being used for the development of nanometer scale materials with outstanding potential technological applications [13]. Owing to their structural and electronic uniqueness, carbon nanotubes have been proposed either in advanced electrochemical devices or as molecular-sized electrodes for very fast electrode kinetics research and for sensing and immunosensing.

One promising approach is the direct electrical detection of biological macromolecules using semiconducting nanowires or CNTs configured as field-effect transistors, CNTFETs, which change conductance when charged macromolecules are bound to receptors linked to the device surfaces [14-17]. CNTFET immunosensors have been prepared by joining the antibodies directly to the CNT or through the use of aptamers. Park et al. [18], have immobilized monoclonal antibodies against carcinoembryoic antigen. Chen et al.[19] have developed CNTFETs for biomarker detection for the early diagnosis of cancer. Li et al.[20] have demonstrated a novel FET immunosensor for the

detection of prostate-specific antigen. Utilizing a monoclonal antibody against immunoglobulin (IgE) immobilized in the device, the IgE concentration was estimated using a CNTFET [21]. Likewise, the possibility of a label-free electrical detection of the DNA-hybridization utilizing semiconductor field-effect sensors offers a new approach for a new generation of DNA chips with direct electrical readout for a fast, simple and inexpensive analysis of nucleic acid samples. Poghosian [22] has evaluated the possibilities and limitations of label-free detection of DNA hybridization with field-effect-based devices. The inherent miniaturization of such devices and their compatibility with advanced microfabrication technology make them very attractive for DNA diagnostics.

This paper report a summary of the previously reported [23, 24] label free detection of DNA hybridization and recognition of two anabolic androgenic steroids, using a large array of CNTFET. We present a methodology for avoiding nonspecific DNA adsorption on CNTs using a polymer, Figure 1, anchored to the device and providing at the same time a stable binding for DNA and specific antibodies for Stz and MB through robust amide linkages.

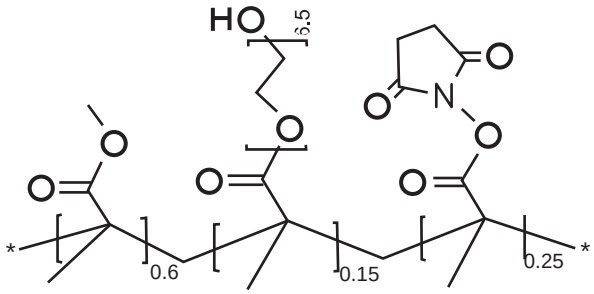

Figure 1. Poly (methylmethacrylate$_{0.6}$-co-poly (ethyleneglycol) methacrylate$_{0.15}$-co-N-succinimidyl methacrylate$_{0.25}$).
Figura 1. Poli (metilmetacrilato$_{0.6}$-co-poli (etileneglicol) metacrilato$_{0.15}$-co-N-succinimidil metacrilato$_{0.25}$).

Anabolic androgenic steroids (AAS) are banned substances in different fields. The World Anti-Doping Agency (WADA) [25] and the European Commission [26] have prohibited the utilization of AAS compounds for enhancing athletic performance and as a growth promoter in cattle owing to their being considered a public health risk. In this paper, we propose the utilization of field-effect transistor arrays based on carbon nanotubes as immunosensors for the detection of stanozolol (Stz) and methylboldenone (MB), Figure 2. Stz and MB are two AAS that are banned by WADA and the European Commission. The methodology used takes advantage of the specifity of the immune assays but with the added value of the electronic measurements being faster and direct. We report and analyze the changes of the electrical CNTFET characteristics upon interaction with the chemicals used for binding the DNA and upon hybridization.

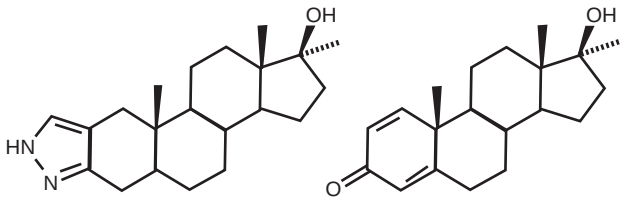

Stanozolol (St) Methylboldenone (MB)

Figure 2. Anabolic steroids: Stanozolol and Methylboldenone (MB).
Figura 2. Esteroides anabolizantes: Estanozolol y Metil-Boldenona.

2. Experimental

The experimental details for the fabrication of the sensors arrays, the synthesis of the polymer and the production of the specific steroids were reported previously [23, 24]. Oligonucleotide NH2-ssDNA (5'-NH2-hexyl-CGAGTCATTGAGTCATCGAG-3') and its complementary C-ssDNA (5'-CTCGATGACTCAATGACTCG-3') were used. Two strategies were followed for the bonding of the biomelecules in the CNTFET. For the first one, the direct bonding of the DNA and specific antibodies to the CNTs in the CNTFET as represented in Figure 3 was carried out. For the second one, the polymer was bonded to the CNTs no-covalently and afterwards, aminated sequences of DNA and the antibodies were bonded to the transistors by covalent strong amide linkages, Figure 4.

The devices were electrically characterized before and after attaching any chemicals or biomolecules in order to determine their effect on the electrical characteristics of the transistors, and statistical analyses of a large array of devices were performed. Only devices having good transistor behaviour showing on/off current ratio higher than 100 were considered in the study. All the bare devices show p-type or ambipolar transistor behavior.

The parameters of interest are the threshold voltage VTH and the drain-source current IDS at the maximum negative voltage. The threshold voltage VTH is taken as the x-intercept of the line tangent to the steepest part of IDS-VG curve. Because the threshold voltage depends on the sweep direction of the back gate voltage, a separate VTH is extracted for the forward and the reverse sweep.

3. Results and discussion

Figure 5 shows the changes in the I_{DS}-V_G curves in the DNA hybridization process on a typical CNTFET. The plots of the device show how the deposition of the chemicals and biomolecules modify the I_{DS}-V_G

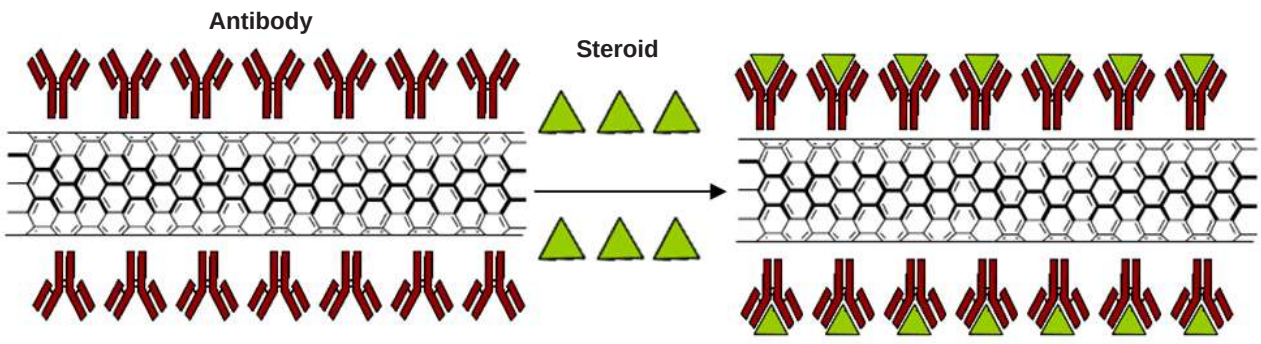

Figure 3. Schematic representation of the bonding of antibodies and steroids to CNTs.
Figura 3. Representación esquemática del enlace de anticuerpos y esteroides a los CNTs.

and/or the V_{TH} characteristics. The polymer was used to prevent non-specific adsorption of the other biomolecules, and the last two steps shown in Figure 5 involve the blocking of excess succinidimyl groups using ethanolamine (EA) blockers, followed by hybridization. It can be seen from Figure 5 an important shift of the VTH with the hybridization as well as significant decrease in I_{DS}.

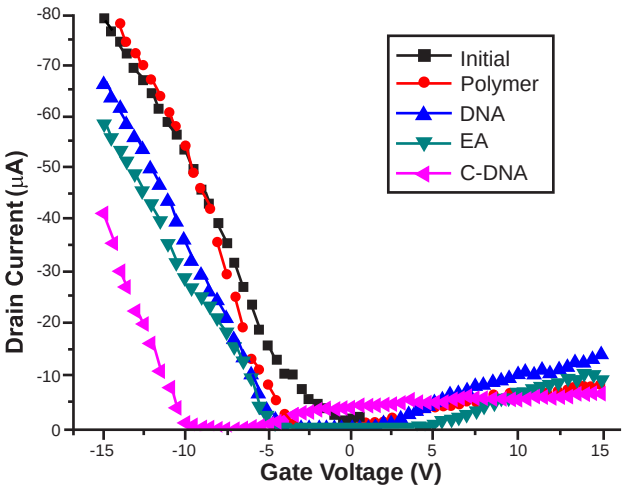

Figure 5. I_{DS}/V_G plots of a typical device for the direct swept of: the bare device, after anchoring the polymer, after simple sequence DNA bonding, after blocking the succynimidil groups with EA and in the hybridization step with the complementary sequence.
Figura 5. Curvas I_{DS}/V_G de un dispositivo típico para el barrido directo de: el dispositivo de partida, después del anclaje del polímero, después del enlace de la secuencia simple de ADN, bloqueo de los grupos succinimidil con EA y en la hibridación de ADN.

Likewise, when the forward and reverse sweep are considered, it was determined [23] a large increase in the hysteresis in the I_{DS}/V_G curves following DNA hybridization. The shift of V_{TH} to more negative values for the forward sweep (V_G from -15V to +15V) indicates electron traps, whereas the shift to more positive values for the reverse sweep (V_G from +15V to -15V) is evidence of holes trap. It is known that both electron and hole transport can occur on a double strand DNA, with holes hopping on guanine and adenine bases, and electrons on cytosine and thymine bases [27].

Regarding the steroids recognition, Figure 6 shows the I_{DS}/V_G plots for the recognition step when the antibodies are bonded to the polymer. When polymer is used to bond the antibodies, the changes in IDS are statistically significant for the forward and reverse steps in the absence of polymer in Stz recognition and in the presence of polymer for the MB recognition. The presence of polymer reduces considerably the hysteresis and the contribution of SB as indicated by the reduction of the changes in the mean IDS values in Stz recognition. In the MB recognition in the absence of polymer, the changes in IDS are very low probably because the changes in SB are balanced by those of the scattering potential. The presence of polymer seems to prevent the changes in SB and makes visible the changes in IDS probably due to potential scattering for the MB recognition.

With regard to the mechanism of detection in the absence of polymer, several overlapped mechanisms could be present. In addition to charge transfer, scattering potential and SB modification reported by other authors [28] electron and hole trap mechanisms with hysteresis decrease in the absence of polymer, and hysteresis increase in the presence of polymer have been determined as for the electronic detection of DNA hybridization.

In the presence of polymer, the changes in SB are possibly of low relevance, making the scattering mechanism and charge transfer the predominant detection mechanisms.

The bonding of the polymer with the CNTFETs prevents the nonspecific adsorption of the steroids such as nantranone and antibodies on the CNTFETs, but it has been determined that streptavidin causes statistically significant changes, indicating nonspecific adsorption to the polymer or some kind of conformational changes that produce electron transfer in the transistor. Nonspecific binding is a big challenge particularly in the immunoassay field.

4. Conclusions

The electronic detection of the DNA hybridization has been carried out by using a large array of CNTFETs. The method uses a synthetic polymer that is well adsorbed to the walls of CNT and carries activated succinimidyl ester groups used to fix the NH2-ssDNA probes. This method of anchoring the probe DNA can prevent the nonspecific adsorption of DNA molecules onto the CNTFET that can occur by virtue of aggregation on the sidewalls of the contact electrodes. The mechanism of the CNTFETs' electrical response is changed significantly by the utilization of the polymer. DNA hybridization produced statistically significant changes in the threshold voltages reflecting the charge trapping character of hybridized DNA. Through these observations it has been possible to detect the charge transfer inherent to the hybridization reaction.

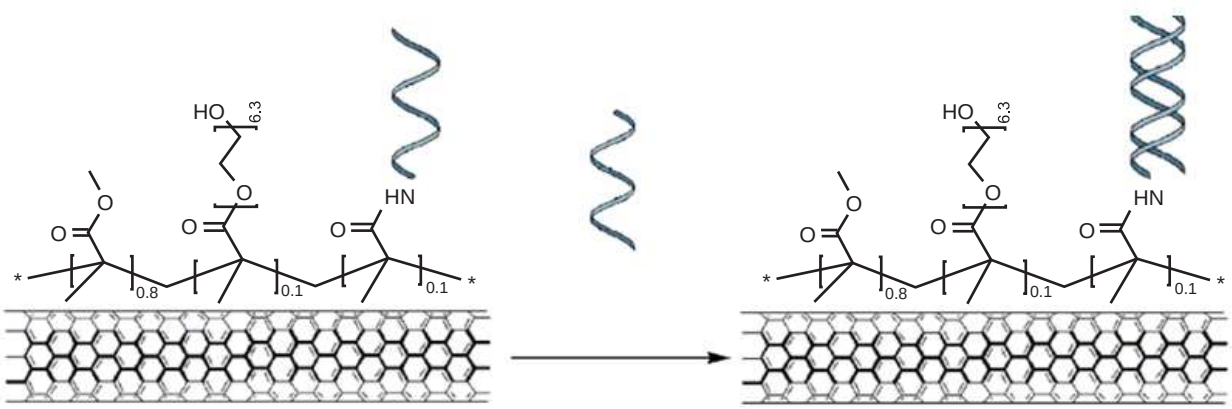

Figure 4. Schematic representation of the DNA hydridization after bonding the aminated DNA single sequence to the polymer in the CNTFET.
Figura 4. Representación esquemática de la hibridación de ADN después del enlace de la secuencia simple de ADN aminada al polímero.

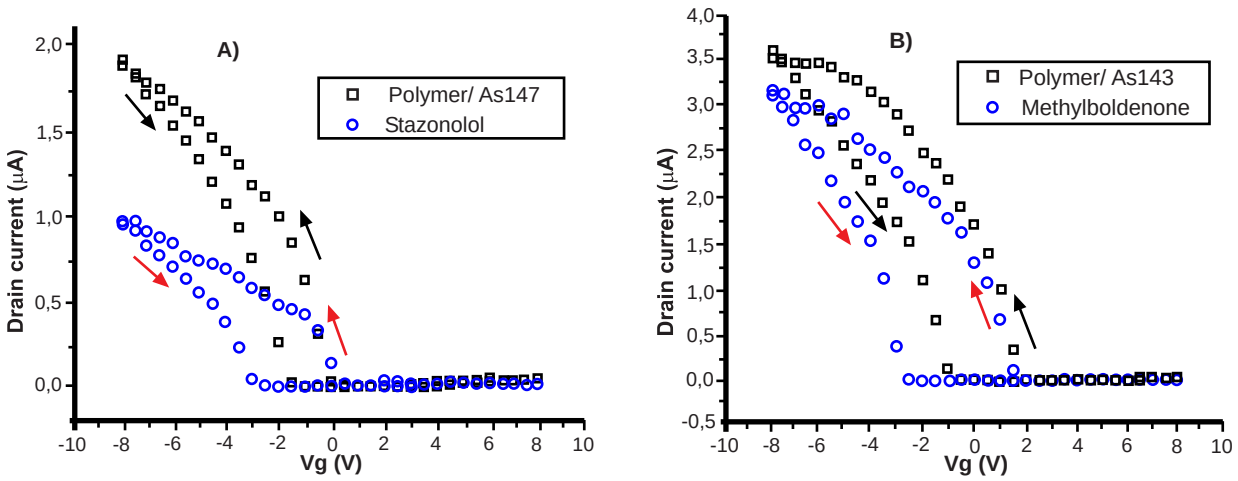

Figure 6. I_{DS}/V_G plots of typical CNTFETs. (A) After anchoring the polymer and As147 antibody (black) specific for Stz and after anchoring stanozolol (blue). (B) After anchoring the polymer and As143 antibody (black) specific for MB and after anchoring methylboldenone (blue).
Figura 6. Curvas I_{DS}/V_G de un CNTFET representativo. (A) Después del anclaje del polímero y el anticuerpo , As147, especifico para el Stz (negro) y después del anclaje de Stz (azul). B) Después del anclaje del polímero y el anticuerpo As 143, específico para la MB (negro) y tras el enlace con la MB (azul).

The feasibility of electronic detection of two anabolic steroids, stanozolol and methylboldenone, has been demonstrated using CNTFET transistors. The bonding of Stz and MB to the specific antibody produces strong changes in the electrical properties of the CNTFET, showing statistically significant changes in the Vth in the forward and reverse sweeps in the recognition step when the antibody is attached directly to the CNT and changes in the forward sweep of the recognition step when the antibody is bonded with the polymer, indicating charge transfer mechanism.

As far as the specificity of the detection is concerned, it has been determined that the CNTFETs do not show statistically significant changes when the antibodies are in contact with other steroids such as nantranone; nevertheless, cross-reactivity with other steroids will have to be studied more exhaustively. The data reported represent a proof of concept of the feasibility of electronic steroid immune detection. Nevertheless, further research needs to address the development of practical biosensors that prevent nonspecific adsorption of biomolecules such as streptavidin on CNTs and enable direct detection, thus avoiding the necessary separation steps when serum samples are used.

5. Acknowledgments

This work has been supported by the Spanish MEC Project NAN2004-09415-C05-05 and by the Molecular Foundry LBNL, Project 126. Work at the Molecular Foundry was supported by the Office of Science, Office of Basic Energy Sciences, of the U.S. Department of Energy under Contract No. DEAC02-05CH11231.

6. References

[1]Gordon AT, Lutz GE, Cooper RA, Boninger ML. Introduction to Nanotechnology: Potential Applications in Physical Medicine and Rehabilitation. Am. J. Phys. Med. Rehabil. 2007, 86, 225–241.

[2]Riehemann K, Schneider SW, Luger TA, Godin B, Ferrari M, Fuchs H. Nanomedicine. Challenges and Perspectives. Angew. Chem., Int. Ed. 2009, 48, 872–897.

[3]Datta M, Malhotra B D, Pandey P. Prospect of Nanomaterials in Biosensors. Anal. Lett. 2008, 41, 159–209.

[4]Patolsky F, Timko BP, Yu G, Fang Y, Greitak AB, Zheng G, Lieber CM. Detection, Stimulation, and Inhibition of Neuronal Signals with High-Density Nanowire Transistor Arrays. Science 2006, 313, 1100–1104.

[5]Ainslie K, M, Desai TA. Microfabricated Implants for Applications in Therapeutic Delivery, Tissue Engineering, and Biosensing. Lab Chip 2008, 1864–1878.

[6]Chaniotakis N, Sofikiti. N. Novel semiconductor materials for thr development of chemical sensors and biosensors. A review Anal. Chim. Acta 2008, 615, 1-9.

[7]Michalet X, Pinaud FF, Bentolila LA, Tsay JM, Doose S, Li JJ, Sundaresan G, Wu AM, Gambhir SS, Weiss S. Quantum dots for Live Cells, in Vivo Imaging, and Diagnostics. Science 2005, 307, 538-544.

[8]Reinhard BM, Siu M, Agarwal H, Alivisatos AP, Liphardt J. Calibration of Dynamic Molecular Rulers Based on Plasmon Coupling between Gold Nanoparticles. Nano Lett. 2005, 5, 2246-2252.

[9]Bunimovich YL, Shin YS, Amori M, Kwong G, Heath JR. Quantitative real-time measurements of DNA hybridization with alkylated nonoxidized silicon nanowires in electrolyte solution. J. Am. Chem. Soc. 2006, 128, 16323-16331.

[10]Jimenez J, Sheparovych R, Pita M, Narvaez Garcia A, Dominguez E, Minko S, Katz E. Magneto-induced self-assembling of conductive nanowires

for biosensor applications J. Phys. Chem. C 2008, 112, 7337-7344.

[11]Tans SJ, Verschueren ARM, Dekker C. Room-temperature transistor based on a single carbon nanotube. Nature 1998, 393, 49-52.

[12]Allen BL, Kichambare PD, Star A. Carbon Nanotube Field-Effect-Transistor-Based Biosensors. Adv. Mater. 2007, 19, 1439–1451.

[13]Paolucci D, Marcaccio M, Paolucci F, Lurlo M. Electron Transfer in Pristine and Functionalised Single-Walled Carbon Nanotubes. Chem. Commun. 2008, 4867–4874.

[14]Cui Y, Wei Q, Park H, Lieber CM. Nanowire Nanosensors for Highly Sensitive and Selective Detection of Biological and Chemical Species. Science 2001, 293, 1289–1292.

[15]Hahm J, Lieber CM. Direct Ultrasensitive Electrical Detection of DNA and DNA Sequence Variations Using Nanowire Nanosensors. Nano Lett. 2004, 4, 51–54.

[16]Chen RJ, Bangsaruntip S, Drouvalakis KA, Kam NWS, Shim M, Li YM, Kim, W, Utz PJ, Dai H. Noncovalent Functionalization of Carbon Nanotubes for Highly Specific Electronic Biosensors. Proc. Natl. Acad. Sci. U.S.A. 2003, 100, 4984–4989.

[17]Chen RJ, Choi HC, Bangsaruntip S, Yenilmez E, Tang XW, Wang Q, Chang YL, Dai HJ. An Investigation of the Mechanisms of Electronic Sensing of Protein Adsorption on Carbon Nanotube Devices. J. Am. Chem. Soc. 2004, 126, 1563–1568.

[18]Park DW, Kim YH, Kim BS, So HM, Won K, Lee JO, Kong KJ, Chang H. Detection of Tumor Markers Using Single-Walled Carbon Nanotube Field Effect Transistors. J. Nanosci. Nanotechnol. 2006, 3499–3502.

[19]Chen RJ, Bangsaruntip S, Drouvalakis KA, Kam NW, Shim M, Li Y, Kim W, Utz PJ, Dai, H. Non-covalent Functionalization of Carbon Nanotubes for Highly Specific Electronics Biosensors. Proc. Natl. Acad. Sci. U.S.A. 2003, 100, 4084–4989.

[20]Li CM, Lin H, Lei B, Ishikawa F, Datar R, Cote R, Thompson M, Zhou C. Complementary Detection of Prostate Specific Antigen Using In2O3 Nanowires and Carbon Nanotubes. J. Am. Chem. Soc. 2005, 127, 12484–12485.

[21]Maehashi K, Katsura T, Kerman K, Takamura Y. Matsumoto K, Tamiya E. Label-Free Protein Biosensor Based on Aptamer-Modified Carbon Nanotube Field-Effect Transistors. Anal. Chem. 2007, 79, 782–787.

[22]Poghossian A, Cherstvy A, Ingebrandt SA, Offenhausser A, Schöning MJ. Sens. Actuators, B 2005, 111, 470-480.

[23]Martínez MT, Tseng YC, Ormategui N, Loinaz I, Eritja R, Bokor J. Label-Free DNA Biosensors Based on Functionalized Carbon Nanotube Field Effect Transistor. NANOLETERS, 9, 2, 2009, 530-536.

[24]Martínez MT, Tseng YC, Salvador JP, Marco MP, Ormategui N, Loinaz I, Bokor J. Electronic anabolic steroids recognition with carbon nanotubes field effect transistors. ACSnano, 2010,4, 3, 1473-1480.

[25]WADA in http//:www.wada-ama.org/.

[26]EC (1996) Directive 96/23/EC; Off. J. Eur. Commun, L 125, 3, COUNCIL DIRECTIVE of 29 April 1996 on measures to monitor certain substances and residues thereof in live animals and animal products and repealing. Directives 85/ 358/EEC and 86/469/EEC and Decisions 89/187/EEC and 91/664/EEC.

[27]Cordes M, Giese, B. Electron transfer in peptides. Chemical Society Reviews, 2009, 38, 892-901.

[28]Allen BL, Kichambare PD, Star A. Carbon Nanotube. Field-Effect-Transistor-Based Biosensors. Adv. Mater. 2007, 19, 1439–1451.

New Strategies for the Selective Functionalization of Carbon Materials

Nuevas Estrategias para la Funcionalización Selectiva de Materiales Carbonosos

M. Pérez-Mendoza[1]

Grupo de Investigación en Solidos Porosos, Departamento de Química Inorgánica, Facultad de Ciencias, Universidad de Granada, 18071 Granada, España

Abstract

Selectively surface-modified solids can play a crucial role in the development of new materials devised to give effective answers to the new technology demands of the more sustainable 21st-century industry. This has brought about a concentration of research efforts on the elaboration of specific chemical functionality on solid surfaces. Nevertheless, the introduction of specific surface functionalization on carbon materials has not yet realized the degree of sophistication and control that other solid materials have reached. This article reviews the latest research developed under the CARB-NANOMETAL project (at the Universities of Granada and Jaén) towards the designing of new strategies for the selective functionalization of carbon materials.

Resumen

Los materiales sólidos funcionalizados superficialmente de forma selectiva pueden jugar un papel fundamental en el desarrollo de nuevos materiales que den respuestas a las nuevas demandas tecnológicas de las, cada vez más sostenibles, industrias del siglo XXI. No obstante, la funcionalización selectiva de materiales carbonosos no ha alcanzado todavía el nivel de sofisticación y control que sí se ha conseguido en otros materiales. Este artículo hace una revisión de las últimas investigaciones llevadas a cabo en las Universidades de Granada y Jaén, en el marco del proyecto CARB-NANOMETAL.

1. Introduction

The functionalization of carbon materials has become a key issue for materials science researchers in the latest years. It is well known that the behaviour of carbon materials can vary from side to side depending on their surface chemistry. Therefore to control the introduction of functionalities onto carbon surfaces, in a selective and homogeneous way, can be the doorway to find new applications for carbon materials and to tackle some of the targets set by industry. This is even more relevant for carbon nanotubes, where the surface chemistry can condition the solubility in different media, the electronic behaviour and the mechanical properties, and where the external surface area/bulk ratio is higher than in other carbon materials. For example, the capability of the tubes to be dispersed in aqueous media is crucial for their use in bio-applications like drug delivery or biomaterials. Another large field of potential application for selective-functionalized carbon materials is their use as chemical sensors and complexants for selective ion recovery.

Last years, at the Department of Inorganic Chemistry of the University of Granada and at the Department of Inorganic and Organic Chemistry of the University of Jaén, we have been developing new strategies to selectively functionalize different type of carbon materials (active carbons, carbon nanotubes and carbon blacks) by selectively fixing organic functions to their surface. The aim is preparing hybrid materials that can act as good and selective metal ion scavengers in aqueous solutions, susceptible of being subsequently reduced to obtain metal nanoparticles. The selective metal ion retention is achieved by introducing selective metal ligands centres in the anchored organic functions.

Two different approaches to produce a selective and homogeneous functionalization have been explored. The first one is based on creating a π-π interaction between the arene centres existing on the graphite microcrystals of the carbon material and a conveniently functionalized pyrimidine ring bonded to the metal receptor part of the organic function (Figure 1). The second one is based on establishing covalent bonds between a dendritic organic molecule, with metal complexing units, and the carbon surface. This is achieved through previously introduced reactive heteroatoms or functions at the surface, i.e., using reactive functionalities as primary groups to subsequent anchoring of complex organic functions as secondary functionalization (Figure 2). In this communication, we review our latest results on both

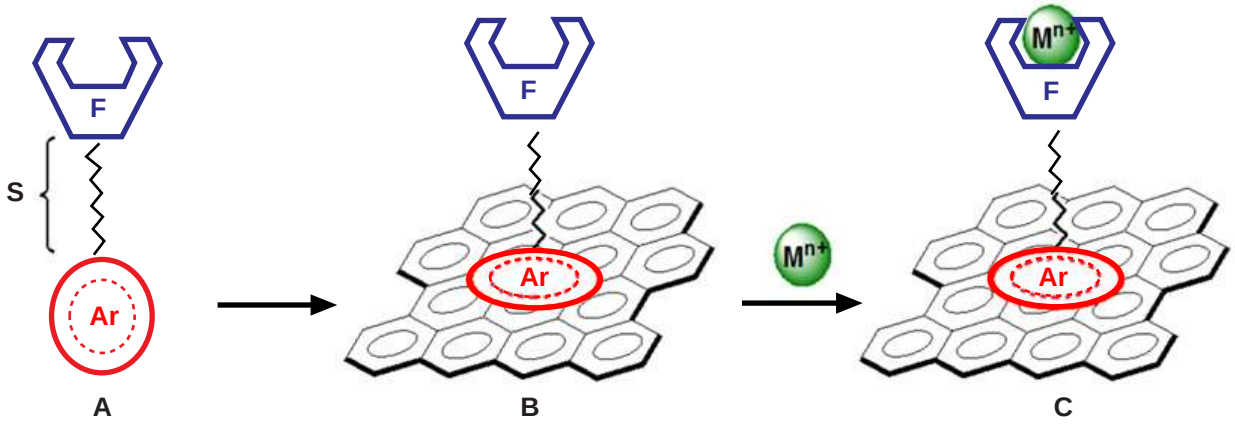

Figure 1. Functionalization using a selective molecular receptor.

1 For detailed authorship see acknowledgements section.

methodologies, which can be easily extrapolated to other organic functions and other type of carbon materials.

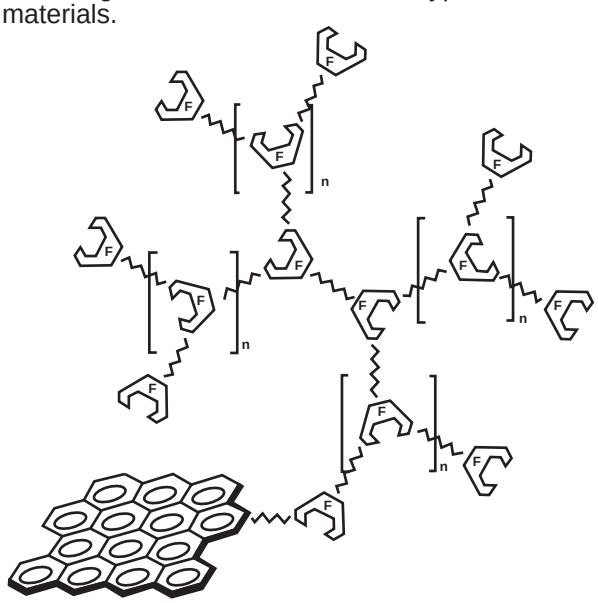

Figure 2. Functionalization using a polyfunctional molecular receptor.

2. Functionalization with molecular receptors by π-π stacking interaction

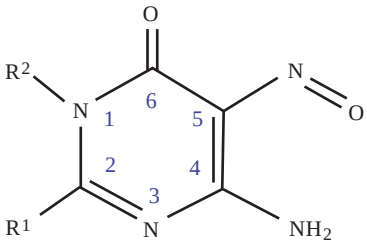

Figure 3. Structure of the pyrimidine moiety.

As mentioned in the introduction section this approach, originally developed at the Department of Inorganic and Organic Chemistry of the University of Jaén, is based on the anchorage of organic molecules to the graphite sheets of the carbon surface. These organic molecules (from now on, receptors) are based on a pyrimidine moiety that has in C2 a polymethylene chain with different functions (F), which can behave as selective metal ligands (Figure 3). The anchorage takes place by, among others, π-π interaction (stacking) between the pyrimidine moiety of the chemical receptor and the arene centres of the graphite planes. Thus, it was proposed that not only dispersive forces, but also electrostatic and these p interactions contribute to the adsorbate-adsorbent interaction.[1,2]. The electrostatic contribution is the result of negative charge of the quadrupole moment of the arene centres and the positive charge of the aromatic moiety of the receptors, while the π-π stacking is an electronic donor-aceptor interaction. This interaction has been corroborated by XPS analysis of the molecular receptors before and after adsorption, showing a shift in the N 1s band towards lower binding energies. The result of these relatively strong interactions is that the adsorption of the receptors on the carbon surface is highly irreversible [3]. Therefore, this procedure allows obtaining very stable carbon/receptor hybrid materials. Moreover, these hybrid materials have two additional advantages: i) a rather specific and selective functionalization of the surface, provided by the F functions, and ii) a very homogeneous functionalization evenly dispersed through the whole surface. It is worth mentioning that this procedure does not require a primary introduction of chemical groups on the surface of the carbon material.

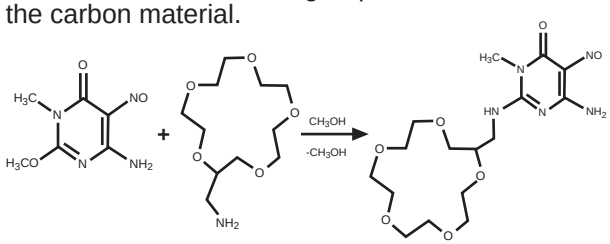

Figure 4. Preparation of the 15-crown-5 molecular receptor.

The C2 position of the pyrimidine moiety (Figure 3) presents a very remarked low electron density, which facilitates nucleophilic attacks by amines or other similar nucleophiles. Therefore, it is relatively easy to attach different organic functions with a hydrophilic character to the C2 position of the pyrimidine ring. This allows us to design and prepare selective molecular receptors for targeted metal ions depending on the complexing properties of the functional units (F) of the organic fragments [4]. An aliphatic chain (S) is used as a separator. The charge variation in F can give the receptor great versatility regarding the type of ion we want to adsorb.

In previous works, good adsorption capacity for metallic ions was achieved by using aminoacidic fragments as F, and supporting the organic function on the surface of a commercial activated carbon [4,5]. Those works clearly evidenced that the metal ion adsorption was taking place at the F function and that the capacity was substantially improved

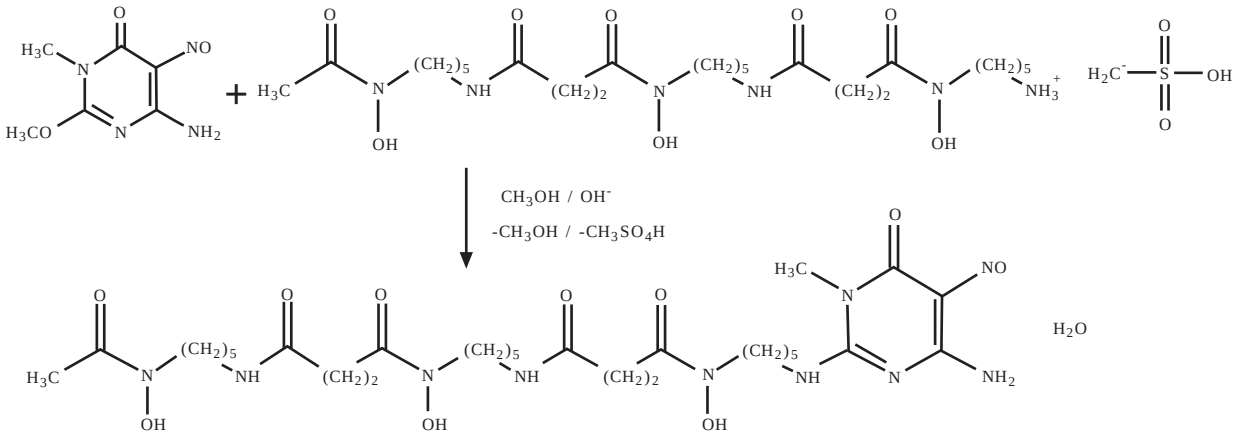

Figure 5. Preparation of the desferroxiamine-b (DFB) molecular receptor.

with regard to the original active carbon. Following the same methodology [6,7], new more selective functional units have been designed recently in order to prepare hybrid materials with improved selectivity. For example, we obtained a receptor with a crown ether function in the C2 position (Figure 4) due to the selectivity that the crown ether macrocycle can offer depending on the size of the metal ion [8,9]. The crown ethers are also very flexible molecules, capable to adapt to different coordination environments and reaction media. Another receptor prepared is based on the desferroxiamine-B (DFB) (Figure 5), due to its high affinity for metal ions with acid Pearson character, like iron, aluminium or gallium [10,11]. Both receptors have been irreversibly anchored to the surface of two different activated carbons. The amount of receptor fixed can be tuned by varying the concentration of the receptor and the pH of the solution [4,12]. In all cases, the hybrid materials prepared resulted very stable and with a remarkable improved adsorption capacity for metal ions compared to the original carbon material (Figure 6).

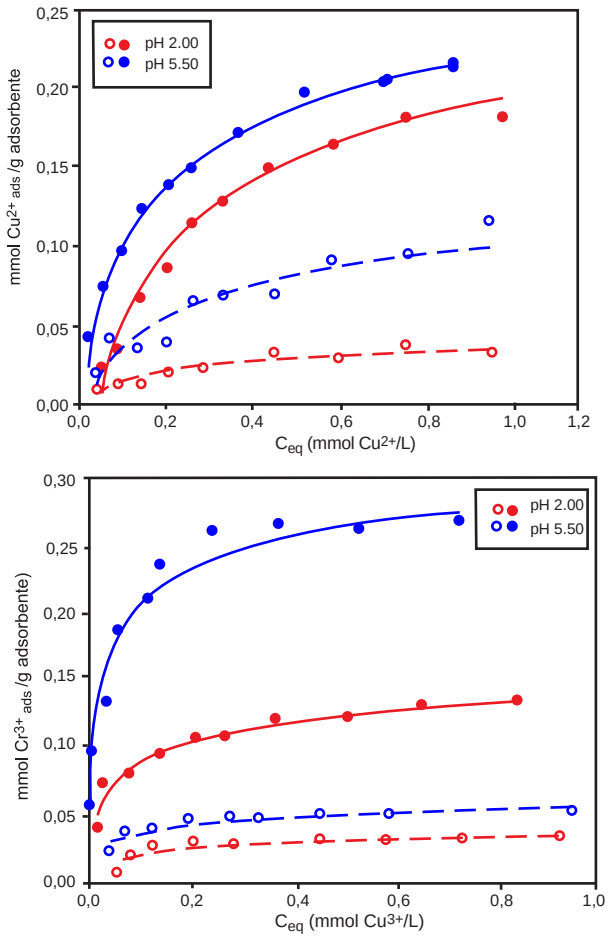

Figure 6. a) Cu^{2+} adsorption isotherms on Merck-15-crown-5 hybrid material (solid symbols) and carbon Merck (empty symbols); b) Cr^{3+} adsorption isotherms on F-DFB hybrid material (solid symbols) and carbon F (empty symbols).

Nevertheless, the most remarkable result of such work is that the metal adsorption is directly related to the ion affinity of the free receptors in solution [4,12]. For a defined ligand and at a fixed pH, the adsorption capacity X_m increases linearly with the effective constant, K_{eff}, which is related to the thermodynamic nature of the metal-ion receptor interaction. Thus, a higher selectivity of the receptor for a certain metal ion (higher value of K_{eff}) results in a larger maximum adsorption capacity for that ion of a hybrid material with that supported receptor. This means that we are succeeding in transferring the complexing properties of the functional centres to the carbon surface. Such result can have important implications in the design of new selective hybrid materials, as it is feasible to predict the metal ion adsorption capacity based on the affinity constants of the receptors in solution.

Another relevant result of this work relates to the effect of the porosity. Although this factor is less important in carbon nanotubes and carbon blacks, it turns crucial when the support is an active carbon with a well-developed porous texture. The results found using activated carbons with different textural characteristics point out that the existence of a wide range of porous sizes, with wide mesopores and a significant amount of macropores, increases the efficiency of the functionalization, even for carbon materials with lower total pore volumes and lower surface areas. The functions fixed in the narrow microporosity block the access to inner pores, resulting in hybrid materials with lower amounts of supported molecular receptors. Moreover, the porous texture has also critical importance in the complexation capability of the organic functions. For example, results for Cu^{2+} adsorption allow us to conclude that a considerable amount of the molecular receptors adsorbed in narrow micropores are forced to adopt conformations that are not adequate for the coordination with the metal ions. In the case of the hybrid materials based on an activated carbon with mainly narrow micropores, this results in lower Cu^{2+} adsorption capacities than the parent AC material. Therefore, a well-developed network of pores, with large pores and good accessibility, is more important for the efficiency of the functionalization and the performance of the hybrid materials than higher specific surface areas and micropore volumes.

3. Functionalization with polyalkylamines by covalent bonding to the carbon surface

The second approach considers the preparation of new effective and stable metal-scavenging hybrid materials based on rigid, non-swelling and chemically inert carbon supports, which can range from active carbons to carbon nanotubes. In particular, we have focused in Pd^{2+} recovery. The scarcity of palladium in the earth crust and the location of its sources in a very few territories have made palladium recovery and recycling a highly strategic and economic issue tackled in the general policies of developed countries [13]. Palladium scavenging, apart from being a valuable strategy for recovery, has become an important subject since the transference of a large collection of advantageous palladium catalyzed synthetic procedures from laboratory to the large-scale industrial production depends on the availability of efficient palladium scavengers capable of removing metal traces from the final products. A significant instance of this situation is the fabrication of active pharmaceutical ingredients (API), for which the strict regulation relative to their content in transition metals hampers the use of more efficient metalcatalyzed synthetic procedures [14,15]. Then, large-scale application of transition metal-catalyzed synthetic processes in APIs production requires efficient methods to remove metal residues, especially palladium [16]. Different scavenging techniques have been applied to particular cases [17,18], but retention with solid sorbents constitutes the preferred approach to the problem [16,19]. Among them, chelant resins and surface modified silicas (some currently

commercialized for such purpose) seem to offer the best behaviour in terms of stability and loading capacity, while classical adsorbents as activated carbons have rendered much poorer results [20].

For this purpose, a flexible, water compatible, stable, organic complexant was covalently linked to the carbon surface. Hyperbranched polyethyleneimine (HBPEI) was chosen as the complexant component due to the excellent Pd^{2+} complexing properties. These properties were tested by characterising the system HBPEI/Pd^{2+} in aqueous solution by potentiometric titration methods. The results revealed the formation of very stable complex species between Pd^{2+} and HBPEI, where the effective complexing units were the ethyleneimine trimers, $(-CH_2-CH_2-N<)_3$ (L in the following) into which the polymer can be divided [21]. The predominant species in the pH range from 1 to 9 were $[PdL]^{2+}$ and $[Pd_2L_2H]^{5+}$, for which $logK_{st}$ values of 31.8 and 28.5, respectively, were measured. Even if this complexing behavior is referred to free HBPEI in aqueous solution, our previous experience on ion retention by carbon-supported complexing agents indicates that the complexation behavior after anchorage onto the solid support is closely parallel that observed for the same free complexing agents in solution [2,22], as already commented in the previous section.

The preparation of the new hybrid materials (Figure 7) consisted in a three-stepped procedure: i) oxidation, ii) esterification and iii) grafting of the polychelatogen HBPEI to the carbon material surface through a carboxamide bond with the ester intermediate. In the oxidation step, it is necessary to introduce a considerable amount of carboxylic functionalities on the surface to be subsequently transformed into methyl esters. For this purpose, we have used classical oxidation methods, like HNO_3 oxidation, but also other oxidising techniques like ozonisation and oxygen plasma treatment. The three treatments succeeded in increasing the amount of carboxylic functions on the surface. Particularly, ozonisation treatments, both in solution and in gas phase, rendered good results with oxygen surface concentrations over 8%. It is worthy to note that the procedures to prepare the new material follow a good observance of the green chemistry practices, since only preferred solvents [23], namely water and methanol, are employed, and a direct transformation of esters into amides is conducted.

Several factors influencing the efficiency of the grafting reaction were analyzed, including reaction solvent, temperature, HBPEI/carbon-material mass ratio, reaction time and HBPEI average molecular weight. When a commercial activated carbon F (Filtracarb-SKI 8X30) is used as support, a very efficient grafting of low molecular weight HBPEI (Mn = 600) was achieved, so giving a hybrid material, F-HBPEI, with an 8.4% of nitrogen (measured after thoroughly washing with boiling methanol for 24 h in a Sohxlet extractor), i.e. it is constituted by a 26% (w/w) of HBPEI and a 74% of carbon structural support. Extraction for 24 h in a Sohxlet with boiling water only reduced its nitrogen content to 7.1% what gives an idea of the good stability of this material. The precursors, intermediates and polyamine-grafted materials were characterized by elemental analysis, XPS and solid state DP-MAS ^{13}C NMR. The XPS data afforded, in the case of F-HBPEI hybrid sample, an amine/amide nitrogen atoms ratio of 83:17, i.e. almost half of the terminal amine groups of HBPEI (41% according to quantitative ^{13}C NMR) formed carboxamide linkages with the carbon support. Thus, considering "typical" HBPEI molecules with MW = 600, so containing 14 N atoms in their structures, they should be linked to the surface through 2-3 amide bonds as average. This result is important as, increasing the anchorage points of the polyamine, we are increasing the stability of the organic functionalities on the carbon surface. Such stability is crucial when applying these functional materials in certain applications like selective metal-ion complexation.

The interest of this new materials derives from the variety of capabilities that its surface functionalization offers since (a) it changes the carbon surface into water-compatible, (b) provides the carbon surface with reactive primary and secondary amino groups for further elaboration of the surface functionality,

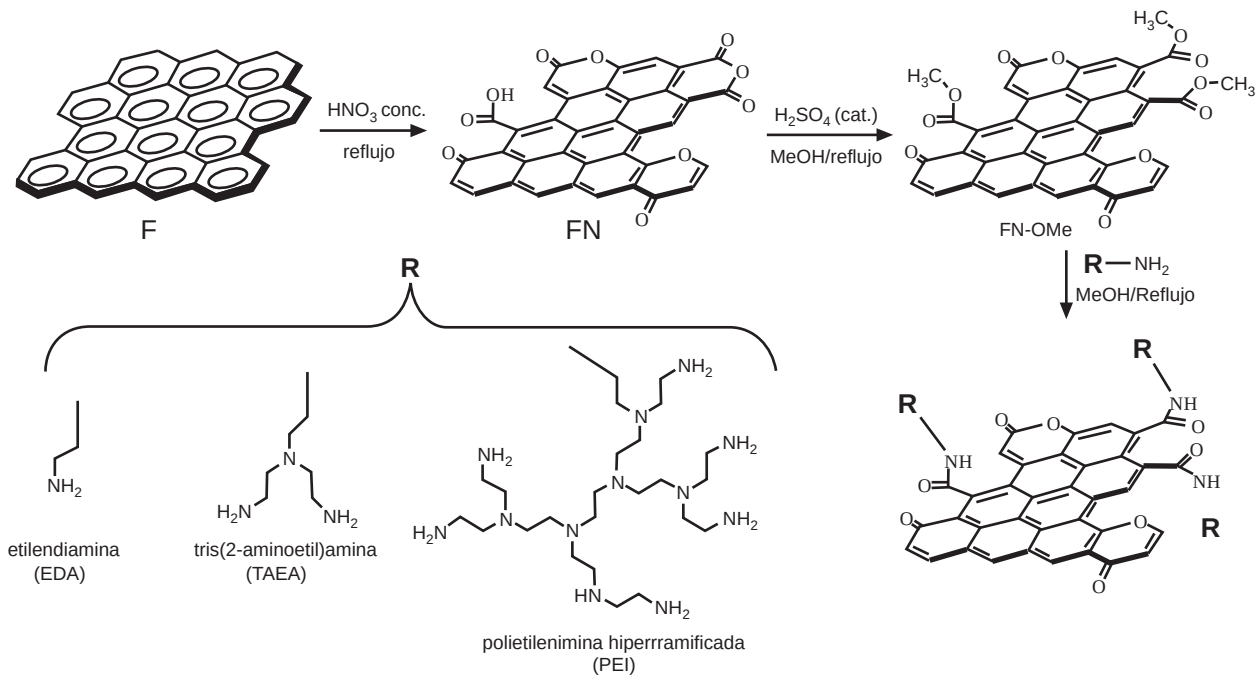

Figure 7. Scheme for the synthesis of carbon-polyamines hybrids.

(c) transforms the carbon into a strong heterogeneous base, (d) provides the carbon surface with an excellent metal-complexing layer because the alkylamino groups are all in relative 1,4 positions placed in a flexible network capable to form stable chelates with transition metal ions, and (e) its easy preparation and scale-up (batches of up to 12.0 g were prepared in our lab) makes it suitable for large-scale applications.

To test the adsorption capacity of the hybrid material based on an active carbon support (F-HBPEI), adsorption experiments of Pd^{2+} solutions (298 K, $[Cl_4Pd]^{2-}$ aqueous solutions at pH 5 and 0.1 M in KCl) were conducted. The isotherms fitted quite well (R^2=0.97) to the Langmuir model with a maximum loading capacity of 1.72 $mmol \times g^{-1}$, which is superior to most of the commercial Pd^{2+} sorbents and comparable with the highest levels retained by some thiol-based scavenging resins[20]. Leaching tests performed in water at pH 5 and pH 1 showed that the full loaded material (1.72 $mmol \times g^{-1}$) losses a minor fraction of metal (4.5% at pH 5 and 13.0% at pH 1), and that there is a loading threshold at 1.33 $mmol \times g^{-1}$ under which no leaching was detected even after 7 days at pH 1 and an ion strength of 0.1 M in KCl. Thus, F-HBPEI is an exceptional scavenger that outperforms previously described materials used for Pd^{2+} removal from aqueous solutions.

In summary, an exceptionally large proportion of a functionality that is very rich in aliphatic polyamines can be efficiently introduced onto carbon surfaces through reliable HBPEI grafting achieved through a straightforward, sustainable and easily scalable procedure. This surface functionality is quite stable and opens a wide variety of interesting applications to the so modified materials due to the versatility of the amine groups. One of such applications is the capture of transition metal ions, which is exemplified by the outstanding performance of F HBPEI as Pd^{2+} scavenger from water solutions.

Different methodologies for the grafting of the polyalkylamines on the surface of different type of carbon materials are also under investigation at present. One possibility to avoid the esterification step and bond the polyamine function directly to the surface is the use of halogen atoms as primary functions. Halogens are well known good leaving groups, which can facilitate the formation of covalent C-N bonds between the nucleophilic attacking amino-group and the carbon surface. Studies using interhalogen compounds in different solvents as halogenating surface agents are being carried out with promising results that reach halogen atomic concentrations over 10% in the surface of carbon nanotubes. Similarly, plasma treatments with halogen derivatives are another way to halogenate carbon surfaces that we are currently exploring. Remarkable halogen surface concentrations have been achieved in the preliminary tests. Similarly, non-destructive reduction methods to transform the captured metal ions into supported nanoparticles are also under study. This would add interesting new possibilities for the already mentioned hybrid materials.

Acknowledgements

This work has been developed under the CARB-NANOMETAL project (MAT2009-14185-C02-01 and MAT2009-14185-C02-02). Funding of the Autonomous Regional Government (J. de Andalucía, Proyecto de Excelencia ref: P09-FQM-4765 and groups RNM342 and FQM273).

The authorship correspond to all the team members, in alphabetical order:

- Research group FQM273. Department of Inorganic and Organic Chemistry (University of Jaén): P. Arranz-Mascarós, C. García-Gallarín, M.L. Godino-Salido, M.D. Gutiérrez-Valero, R. López-Garzón, M.D. López-de la Torre, M. Melguizo-Guijarro, A. Peñas-Sanjuán and A. Santiago-Medina.

- Research Group on Porous Solids (RNM342). Department of Inorganic Chemistry (University of Granada): V. Abdelkader-Fernández, M. Domingo-García, F.J. López-Garzón, F. Morales-Lara and M. Pérez-Mendoza.

A. Peñas-Sanjuán, A. Santiago-Medina, V. Abdelkader-Fernández and F. Morales-Lara acknowledge the financial support in form of predoctoral grants.

6. References

1 Gutierrez-Valero, M. D.; Godino-Salido, M. L.; Arranz-Mascaros, P.; Lopez-Garzon, R.; Cuesta, R.; Garcia-Martin, J. Adsorption of designed pyrimidine derivative ligands on an activated carbon for the removal of Cu(II) ions from aqueous solution. *Langmuir* **2007**, 23, 5995.

2 Garcia-Martin, J.; Godino-Salido, M. L.; Lopez-Garzon, R.; Gutierrez-Valero, M. D.; Arranz-Mascaros, P.; Stoeckli-Evans, H. Adsorption of metal ions on an activated carbon/L-lysine derivative hybrid compound. *Eur. J. Inorg. Chem.* **2008**, 1095.

3 Garcia-Martin, J.; Lopez-Garzon, R.; Godino-Salido, M. L.; Gutierrez-Valero, M. D.; Arranz-Mascaros, P.; Cuesta, R.; Carrasco-Marin, F. Ligand adsorption on an activated carbon for the removal of chromate ions from aqueous solutions. *Langmuir* **2005**, 21, 6908.

4 Santiago-Medina, A. PhD Thesis, Uniersity of Jaén, 2011.

5 Arranz, P.; Bianchi, A.; Cuesta, R.; Giorgi, C.; Godino, M. L.; Gutierrez, M. D.; Lopez, R.; Santiagot, A. Binding and Removal of Sulfate, Phosphate, Arsenate, Tetrachloromercurate, and Chromate in Aqueous Solution by Means of an Activated Carbon Functionalized with a Pyrimidine-Based Anion Receptor (HL). Crystal Structures of $H_3L(HgCl_4)$ center dot H_2O and $H_3L(HgBr_4)$ center dot H_2O Showing Anion-pi Interactions. *Inorg. Chem.* **2010**, 49, 9321.

6 Low, J. N.; Ferguson, G.; Lopez, R.; Arranz, P.; Cobo, J.; Melguizo, M.; Nogueras, M.; Sanchez, A. N-(6-amino-3,4-dihydro-3-methyl-5-nitroso-4-oxopyrimidin-2-yl)glycine-wa ter(1/2). *Acta Crystallogr. Sect. C-Cryst. Struct. Commun.* **1997**, 53, 890.

7 Melguizo, A.; Marchal, A.; Nogueras, M.; Sanchez, A.; Low, J. N. Aminolysis of methoxy groups in pyrimidine derivatives. Activation by 5-nitroso group. *J. Heterocycl. Chem.* **2002,** 39, 97.

8 Cram, D. J. Preorganization - from solvents to spherands. *Angew. Chem.-Int. Edit. Engl.* **1986**, 25, 1039.

[9]Hancock, R. D. Chelate ring size and metal-ion selection - the basis of selectivity for metal-ions in open-chain ligands and macrocycles. *J. Chem. Educ.* **1992**, 69, 615.

[10]Crichton, R. R. *Inorganic biochemistry of iron metabolism*, New York, 1991.

[11]Day, J. P. *Aluminium and other trace elements in renal disease*, Eastbourne, 1986.

[12]Peñas-Sanjuán, A., University of Jaén, 2011.

[13]Critical Raw Materials for the EU. The European Commission.
http://ec.europa.eu/enterprise/policies/raw-materials/files/docs/report-b_en.pdf.

[14]Federsel, H. J. In search of sustainability: process R&D in light of current pharmaceutical industry challenges. *Drug Discov Today* **2006,** 11, 966.

[15]Slagt, V. F.; de Vries, A. H. M.; de Vries, J. G.; Kellogg, R. M. Practical Aspects of Carbon-Carbon Cross-Coupling Reactions Using Heteroarenes. *Org. Process Res. Dev.* **2010**, 14, 30.

[16]Magano, J.; Dunetz, J. R. Large-Scale Applications of Transition Metal-Catalyzed Couplings for the Synthesis of Pharmaceuticals. *Chemical Reviews* **2011**, 111, 2177.

[17]Pink, C. J.; Wong, H. T.; Ferreira, F. C.; Livingston, A. G. Organic solvent nanofiltration and adsorbents; A hybrid approach to achieve ultra low palladium contamination of post coupling reaction products. *Org. Process Res. Dev.* **2008**, 12, 589.

[18]Flahive, E. J.; Ewanicki, B. L.; Sach, N. W.; O'Neill-Slawecki, S. A.; Stankovic, N. S.; Yu, S.; Guinness, S. M.; Dunn, J. Development of an effective palladium removal process for VEGF oncology candidate AG13736 and a simple, efficient screening technique for scavenger reagent identification. *Org. Process Res. Dev.* **2008**, 12, 637.

[19]Garrett, C. E.; Prasad, K. The art of meeting palladium specifications in active pharmaceutical ingredients produced by Pd-catalyzed reactions. *Adv Synth Catal* **2004**, 346, 889.

[20]Won, S. W.; Park, J.; Mao, J.; Yun, Y. S. Utilization of PEI-modified Corynebacterium glutamicum biomass for the recovery of Pd(II) in hydrochloric solution. *Bioresource Technology* **2011**, 102, 3888.

[21]Jarvis, N. V.; Wagener, J. M. MECHANISTIC STUDIES OF METAL-ION BINDING TO WATER-SOLUBLE POLYMERS USING POTENTIOMETRY. *Talanta* **1995,** 42, 219.

[22]Godino-Salido, M. L.; Lopez-Garzon, R.; Arranz-Mascaros, P.; Gutierrez-Valero, M. D.; Santiago-Medina, A.; Garcia-Martin, J. Study of the adsorption capacity to Co(2+), Ni(2+) and Cu(2+) ions of an active carbon/functionalized polyamine hybrid material. *Polyhedron* **2009**, 28, 3781.

[23]Alfonsi, K.; Colberg, J.; Dunn, P. J.; Fevig, T.; Jennings, S.; Johnson, T. A.; Kleine, H. P.; Knight, C.; Nagy, M. A.; Perry, D. A.; Stefaniak, M. Green chemistry tools to influence a medicinal chemistry and research chemistry based organisation. *Green Chem* **2008**, 10, 31.

Interacciones As y Se con cenizas volantes

As and Se interactions with fly ashes

M.A. López-Antón, M. Díaz-Somoano,* M.R. Martinez-Tarazona

Instituto Nacional del Carbón, CSIC. C/Francisco Pintado Fe 26, 33011, Oviedo, España
**Corresponding author: mercedes@incar.csic.es*

Abstract

Arsenic and selenium are toxic elements present in coal in trace concentrations that may be emitted to the environment during coal conversion processes. However, it is possible to retain volatile arsenic and selenium compounds in the fly ashes originated by the process, the proportions retained depending on the characteristics of the ashes and process conditions. This work is focused on the capture of these elements in fly ashes in simulated coal combustion and gasification atmospheres in laboratory scale reactors.

Resumen

El arsénico y el selenio son elementos tóxicos presentes en el carbón en concentraciones del orden de las trazas que pueden ser emitidos al medio ambiente durante los procesos de conversión del carbón. Sin embargo, los compuestos de arsénico y selenio pueden ser retenidos en las cenizas volantes originadas en el propio proceso en distintas proporciones dependiendo de las características de las cenizas y las condiciones del proceso. Este trabajo se centra en la captura de estos elementos en cenizas volantes en una atmósfera de combustión y gasificación de carbón en reactores a escala de laboratorio.

1. Introducción

Algunos de los componentes de la materia mineral del carbón, entre los que se encuentran los elementos traza, se volatilizan durante la combustión y gasificación del carbón. Como consecuencia, la generación de energía a partir del carbón es una de las fuentes antropogénicas de emisión de elementos traza. Entre los elementos definidos como "contaminantes peligrosos" según The Clean Air Amendments (CAAA) de 1990 por la EPA (US Environmental Protection Agengy) se encuentran un total de 11 elementos metálicos que forman parte del grupo de elementos traza en el carbón. Entre estos elementos se encuentran el arsénico y el selenio. Estos elementos traza ocurren naturalmente en la corteza terrestre, sin embargo, en altas concentraciones pueden tener efectos nocivos sobre el medio ambiente y la salud humana.

La creciente preocupación por las emisiones de los compuestos de metales tóxicos desde distintas fuentes industriales y sus efectos sobre el ambiente y la salud pública, ha desembocado en el desarrollo de leyes, directivas y planes de acción orientados al control de sus emisiones. El Consejo de la Unión Europea ha aprobado con fecha 4 de abril de 2001 el Protocolo 1998 al convenio de 1979 sobre contaminación atmosférica transfronteriza a gran distancia en materia de metales pesados [1]. El objetivo del Protocolo es controlar las emisiones de metales pesados, provocadas por las actividades humanas sujetas a desplazamientos aéreos transfronterizos a gran distancia, como son los procesos de combustión y gasificación del carbón.

Las concentraciones de arsénico en el carbón pueden llegar a 100 $\mu g\ g^{-1}$, mientras que el selenio está presente generalmente en concentraciones inferiores a 2 $\mu g\ g^{-1}$. Aunque el conocimiento sobre el comportamiento de los elementos traza en sistemas de gasificación ha sido menos estudiado que en el caso de la combustión, en ambos casos puede esperarse que elementos volátiles y tóxicos tales como As, Se, Sb, Cd, Hg, etc., se encuentren al menos parcialmente en fase gas, o condensados en las partículas de menor tamaño que pueden ser emitidas junto con los gases [2-4]. Algunos autores señalan que las condiciones reductoras de una atmósfera de gasificación pueden originar la formación de algunas especies diferentes a las que se producen en la atmósfera de combustión [5] e incluso se ha sugerido que elementos como arsénico y selenio, que pueden formar hidruros, aumentarían su volatilidad en los procesos de gasificación comparados con los de combustión [6-7].

El comportamiento de las especies de arsénico y selenio, y por tanto, la proporción de especies de estos elementos retenidas en las cenizas volantes durante los procesos de utilización de carbón puede variar en distintas centrales. En términos generales, una alta proporción de arsénico presente originalmente en el carbón se refleja en las partículas de cenizas volantes como resultado de un proceso de condensación o debido a una reacción con algunos de los componentes de las cenizas volantes, mientras que el selenio se escapa en fase gas en proporciones mayores [8].

Recordemos que durante la combustión del carbón la materia mineral presente descompone y se transforma en cenizas. Parte de esta materia mineral queda retenida en la caldera y el resto se arrastra junto con los gases de combustión. Estas cenizas arrastradas por los gases, que son posteriormente retenidas en precipitadores electrostáticos, ciclones filtros de mangas, etc., se denominan cenizas volantes.

Las cenizas volantes representan el mayor porcentaje de los productos de combustión del carbón. Se ha estimado que, de los aproximadamente 65 millones de toneladas de productos de combustión de carbón producidos en Europa en 2003, alrededor del 68% de ellos son cenizas volantes mientras que en los Estados Unidos de América suponen alrededor del 58% de estos residuos [9-10]. La proporción y características de las cenizas volantes producidas en una central térmica, no sólo dependen de las características del carbón sino también del sistema de combustión utilizado y del tipo de caldera, pudiendo llegar en algunos casos a constituir el 90% de la materia mineral originalmente presente en el carbón.

El objetivo final de todos los estudios relacionados con el comportamiento de los elementos traza en los procesos de generación de energía a partir de carbón es reducir sus emisiones manteniendo una alta eficiencia en los procesos de combustión y gasificación. Cualquier mejora en el proceso que implica una captura más eficiente de arsénico y selenio en las cenizas volantes sería un importante paso adelante. Esto se puede conseguir favoreciendo la interacción de los elementos traza con las cenizas, o mediante la reutilización de las cenizas volantes

empleándolas como sorbentes sólidos capaces de adsorber física o químicamente distintas especies gaseosas de estos elementos. En cualquier caso, la utilización de un sorbente determinado en una planta de combustión o gasificación de carbón requiere de un conocimiento profundo sobre todos los aspectos básicos de su comportamiento que permitan el máximo rendimiento. En el presente trabajo se hace un repaso sobre la reducción de especies de arsénico y selenio en fase gas en atmósferas típicas de combustión y gasificación de carbón, utilizando cenizas volantes como sorbentes sólidos, de acuerdo a trabajos realizados anteriormente por los autores en muy diferentes condiciones experimentales. La influencia de distintos parámetros, tales como tipo de proceso de generación de energía a partir de carbón y temperatura en la retención de arsénico y selenio en cenizas volantes serán revisados en las siguientes secciones.

2. Dispositivo experimental

El estudio sobre la retención de arsénico y selenio en distintos sorbentes de cenizas volantes y diferentes condiciones se llevó a cabo en un equipo a escala de laboratorio (Figura 1).

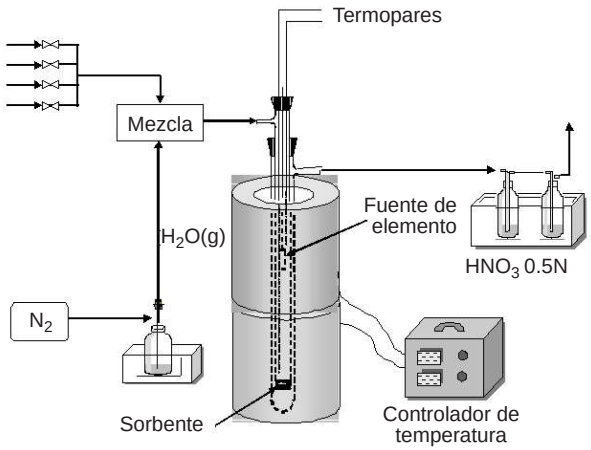

Figura 1. Esquema del dispositivo experimental.
Figure 1. Schematic diagram of the experimental device.

El equipo consta fundamentalmente de un reactor de lecho fijo en el que se encuentra el sorbente y de un sistema capaz de generar una atmósfera similar a la producida en procesos de combustión y gasificación de carbón. (Tabla 1). El elemento en fase gas se obtuvo por evaporación de compuestos puros (As_2O_3 y Se). El sorbente se coloca en el fondo del reactor. Una vez depositado en el lecho, se introduce en el reactor la navecilla con el compuesto puro del elemento traza que se va a utilizar como fuente y se hace pasar la mezcla de gases conteniendo el elemento traza que pasará a través del sorbente a un flujo y durante un tiempo previamente determinados. Una parte del elemento en fase vapor, quedará adsorbido en el mismo y el resto será llevado junto con los gases fuera del reactor, en donde será retenido en unos frascos lavadores colocados a la salida, en los que se comprueba que no se deja escapar el elemento a la atmósfera [11]. Cuando la mezcla gaseosa utilizada en el experimento contiene H2S se incluye un tercer frasco lavador con $Cd(OH)_2$. Finalizado el experimento el sorbente se extrae cuantitativamente del reactor, se muele, se disuelve y analiza mediante espectroscopía de masas de acoplamiento inductivo (ICP-MS) (arsénico) y generación de hidruros acoplado a un ICP-MS (HG/ICP-MS) (selenio) [12].

3. Resultados y discusión

3.1. Retención de arsénico y selenio en cenizas volantes en una atmósfera de combustión

Para este estudio fueron seleccionadas dos cenizas volantes de muy distintas características, no sólo debido a la diferencia del combustible del que proceden sino también al hecho de que se han obtenido en procesos de combustión muy distintos. Por un lado se ha utilizado una muestra de ceniza volante procedente de la combustión de carbón bituminoso muy rico en estériles, en una caldera de lecho fluidizado en la que se utiliza caliza, denominada CTP. Por otra parte se ha empleado una ceniza de una planta de combustión de carbón pulverizado denominada CTA, en la que se utilizan carbones de alto rango como combustibles.

Los experimentos de retención fueron realizados a 120ºC en un flujo de gases de combustión (Tabla 1). Aunque no es un objetivo de este trabajo debemos mencionar que además de arsénico y selenio también se estudió otro elemento de gran interés medioambiental como es el mercurio y por esta razón la temperatura escogida para los experimentos de retención fue de 120ºC. El flujo global de gases utilizado en los experimentos fue de 0.5 l min^{-1} y la concentración de arsénico y selenio en fase gas fue del orden de 0.4 μg ml^{-1}.

En la Tabla 2 y Figura 2 se muestran los resultados obtenidos en las dos muestras de cenizas volantes [13]. La evaluación de los resultados se llevó a cabo utilizando los valores de eficiencia y capacidad de retención. La eficiencia de cada uno de los sorbentes para cada uno de los elementos fue evaluada como el porcentaje de retención, determinado en una serie de experimentos en los que la cantidad de elemento a través del sorbente se fue incrementando sucesivamente. El límite de confianza del porcentaje de retención fue determinado como ±DS (desviación estándar). La capacidad de retención se define como la máxima cantidad de elemento retenida (CRM). Como puede observarse, las CRM fueron superiores con el selenio. Sin embargo las eficiencias fueron similares para los dos elementos. Cuando se comparan las retenciones tanto de arsénico como selenio en la ceniza CTP con las obtenidas en la ceniza CTA, se observan mejores retenciones en la primera, que posee la menor concentración de inquemados expresado como pérdida por calcinación (LOI), pero mayor área superficial. Como ya se demostró en un trabajo anterior [13] la materia carbonosa no es la responsable directa de la captura de arsénico ni de selenio sino fundamentalmente la materia mineral. Cuando las muestras de ceniza post-retención de arsénico fueron analizadas por

Tabla 1. Composición de las mezclas gaseosas (% volumen). **Table 1.** Gas compositions (% by volume).

	%CO	$\%CO_2$	$\%H_2$	$\%O_2$	$\%SO_2$	$\%H_2O$	$\%H_2S$	$\%N_2$
Combustión	----	15	----	9.2	0.2	6.6	----	69
Gasificación	64	3.7	20.9	----	----	4.0	1.0	6.4
Gasificación I	57.6	3.3	18.8	----	----	4.0	----	16.3
Gasificación II	57.6	3.3	18.8	----	----	4.0	1.0	15.3

ablación con láser acoplada a un equipo ICP-MS (LA-ICP-MS) se encontró que el arsénico se encontraba concentrado en las partículas en las cuales el calcio y el hierro estaban presentes. Las especies de arsénico y calcio/hierro podrían reaccionar mediante las siguientes reacciones:

$6CaO + As_4O_{10}(g) = 2Ca_3(AsO_4)_2$ (1) K=1.14x10^{150}
$6CaCO_3 + As_4O_{10}(g) = 2Ca_3(AsO_4)_2 + 6CO_2(g)$ (2) K=1.07x10^{58}
$2Fe_2O_3 + As_4O_{10}(g) = 4FeAsO_4$ (3) K=9.29x10^{33}
$4FeS + As_4O_{10}(g) + 7O_2(g) = 4FeAsO_4 + 4SO_2(g)$ (4) K=1.10x10^{308}

La ceniza CTP presentó un mayor contenido de calcio que justificaría que la retención de arsénico fuera mayor en esta ceniza. Sin embargo, para el selenio no se encontró ninguna correlación entre el calcio y/o hierro con el selenio en una atmósfera de combustión. Estas observaciones sugieran que la retención de selenio en una atmósfera de combustión en las cenizas no tiene lugar mediante una reacción química, o al menos no tiene lugar en una extensión importante. Además cuando las cenizas volantes fueron sometidas a un tratamiento térmico a 120ºC, se produjeron pérdidas de selenio entre el 15 y 20%, indicando que la retención de selenio es parcialmente reversible y por tanto apoyando la hipótesis de que el proceso de retención sea más físico que químico. Sin embargo en el caso del arsénico tras el tratamiento térmico se encontró que el arsénico retenido en las cenizas volantes estaba en una forma estable a la temperatura de 120ºC sugiriendo que retención de arsénico se produce a través de de las reacciones químicas (1-4).

3.2. Retención de arsénico y selenio en cenizas volantes en una atmósfera de gasificación a baja temperatura

La capacidad de las cenizas volantes para la retención de arsénico y selenio en una atmósfera de gasificación a 120ºC, se evaluó utilizando las mismas cenizas (CTA y CTP) que en el caso de la atmósfera de combustión. Las condiciones experimentales fueran las mismas con la excepción de que ahora la atmósfera gaseosa sea reductora en lugar de oxidante (Tabla 1). En la Tabla 3 y Figura 3 se muestran la capacidad de retención máxima y la eficiencia para arsénico y selenio en las cenizas CTA y CTP.

Como se puede observar el comportamiento en una atmósfera de gasificación a baja temperatura fue similar que en una atmósfera de combustión (Tabla 2). Las retenciones son mayores para el selenio que para el arsénico y los mejores resultados fueron obtenidos con la ceniza CTP. De nuevo podemos plantear la hipótesis de que sea alguno de los componentes de la materia mineral el responsable de la retención de estos dos elementos. En el caso del arsénico se pudo observar mediante LA-ICP-MS asociaciones hierro y/o calcio con arsénico en una atmósfera de gasificación.

$4FeS + As_4(g) = 4FeAsS$ (5) K=3.98x10^{14}
$4FeS + As_4S_4(g) + 4H_2(g) = 4FeAsS + 4H_2S(g)$ (6) K=6.00x10^{13}
$2CaO + As_4(g) + 6H_2O(g) = 2Ca(AsO_2)_2 + 6H_2(g)$ (7) K= 2.80x10^{40}
$2CaCO_3 + As_4(g) + 6H_2O(g) = 2Ca(AsO_2)_2 + 6H_2(g) + 2CO_2(g)$ (8) K=2.5x10^{8}

Por tanto la retención de arsénico en cenizas volantes en una atmósfera de gasificación sería fundamentalmente a través de un proceso químico. En el caso del selenio debemos destacar que aunque las máximas capacidades de retención fueron similares en las dos atmósferas, mayores eficiencias fueron encontradas en una atmósfera de gasificación (Tablas 2-3, Figuras 2-3). Según datos teóricos basados en datos de equilibrio termodinámico la especie formada en una atmósfera de combustión es $SeO_2(g)$ mientras que en una atmósfera reductora la especie formada es H_2Se (g) [13]. Por tanto, podría interpretarse como debido a que la cinética se ve favorecida para la especie de selenio presente en la atmósfera de gasificación (H_2Se), pero los centros activos capaces de retener selenio en las cenizas son los mismos. En condiciones reductoras, donde la especie en fase gas esperada es el H_2Se, el análisis mediante LA-ICP-MS confirmó la asociación selenio-calcio/hierro apoyando la hipótesis de la reacción que daría lugar a la formación de CaSe y FeSe en una atmósfera de gasificación (reacciones 8-9), y que no tendrían lugar en condiciones oxidantes de una atmósfera de combustión.

$CaO + H_2Se(g) = CaSe + H_2O(g)$ (9) K=4.07
$FeS + H_2Se\ (g) = FeSe + H_2S(g)$ (10) K=8.97x10^{2}

3.3. Retención de arsénico y selenio en cenizas volantes en una atmósfera de gasificación a alta temperatura

Los sistemas de limpieza de gases en caliente cumplen un doble objetivo, tecnológico, pues se evitan corrosiones, y medioambiental, ya que se minimizan las emisiones. Concretamente en las

Tabla 2. Retención de arsénico y selenio en cenizas volantes en una atmósfera de combustión a 120ºC.
Table 2. Retention of arsenic and selenium in fly ashes in a coal combustion atmosphere at 120ºC.

Sorbente	Surface Area (m^2g^{-1})	LOI %	As		Se	
			CRM mg g^{-1}	Eficiencia %	CRM mg g^{-1}	Eficiencia %
CTA	1.6	5.7	2.83	12±4	15.6	11±2
CTP	6.7	3.8	5.30	17±6	17.8	15±2

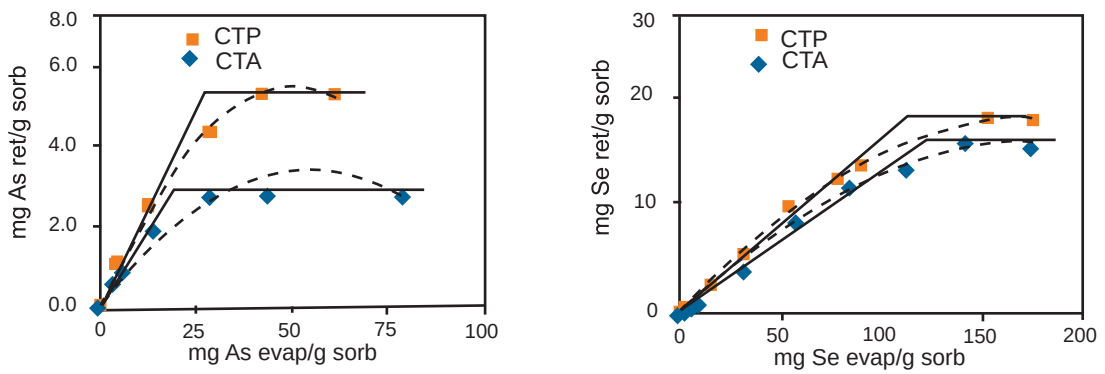

Figure 2. Retención de arsénico y selenio en las cenizas volantes CTA y CTP en una atmósfera de combustión a 120ºC.
Figure 2. Retention of arsenic and selenium in CTA and CTP fly ashes in a coal combustion atmosphere at 120ºC.

Tabla 3. Retención de arsénico y selenio en cenizas volantes en una atmósfera de gasificación a 120ºC.
Table 3. Retention of arsenic and selenium in fly ashes in a coal gasification atmosphere at 120ºC.

Sorbente	Surface Area (m^2g^{-1})	LOI %	As		Se	
			CRM mg g^{-1}	Eficiencia %	CRM mg g^{-1}	Eficiencia %
CTA	1.6	5.7	2.10	12±4	17.4	34±4
CTP	6.7	3.8	4.51	21±5	21.5	35±6

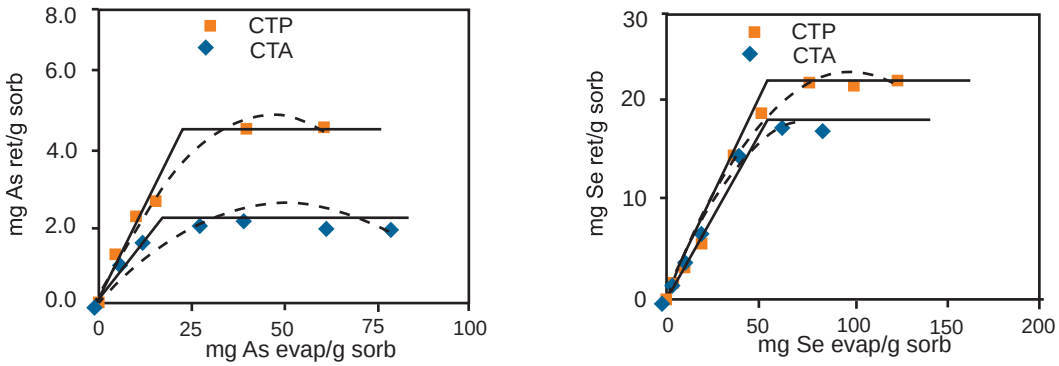

Figure 3. Retención de arsénico y selenio en las cenizas volantes CTA y CTP en una atmósfera de gasificación a 120ºC.
Figure 3. Retention of arsenic and selenium in CTA and CTP fly ashes in a coal gasification atmosphere at 120ºC.

plantas de gasificación integrada de ciclo combinado (GICC) los gases se limpian previamente a su entrada en la turbina. Por ello en este estudio se evaluó también la capacidad de retención de una ceniza volante para especies gaseosas de arsénico y selenio a elevada temperatura. Se utilizó la ceniza CTP y se ensayaron tres temperaturas, 350, 550 y 750 ºC en el caso del arsénico y dos temperaturas, 550 y 750 ºC para el caso del selenio, ya que se necesitó una temperatura superior a 350 ºC para la evaporación del compuesto fuente de elemento. Los experimentos se realizaron en dos atmósferas diferentes, la denominada gasificación I que no contiene azufre en su composición y la mezcla gasificación II, con aproximadamente un 1% de H_2S (Tabla 1).

En ausencia de azufre, la capacidad de retención de arsénico aumenta con la temperatura, alcanzando los 24 mg de arsénico g^{-1} a 750ºC, mientras que en presencia de H_2S (g), a 350 y 550ºC es del mismo orden que en ausencia de azufre disminuyendo, sin embargo a 750ºC (Tabla 4). En lo que se refiere a la cinética de la interacción arsénico-CTP, en la Figura 4 puede verse como la velocidad es máxima a 750 ºC en ambas atmósferas.

Estos resultados sugieren, al igual que sucedía para combustión y gasificación a baja temperatura, la posibilidad de una reacción química. Nuevamente los análisis mediante LA-ICP-MS confirman las asociaciones arsénico-calcio y arsénico-hierro en las muestras post-retención, siendo las reacciones más probables las formuladas anteriormente [5-8].

Las capacidades de retención máximas obtenidas para la retención de selenio con la ceniza volante CTP a alta temperatura (Tabla 5) son del orden de las conseguidas para combustión y gasificación a 120 ºC, siendo mayor la eficiencia y la cinética de la interacción cuanto mayor es la temperatura (Figura 5). En ausencia de azufre se consiguieron retenciones de 25 mg selenio g^{-1} a 550 y 750 ºC. En cambio, cuando la atmósfera contenía H_2S(g), el comportamiento varió con la temperatura, observándose que mientras que a 750ºC la retención era del mismo orden que en ausencia de azufre, a 550ºC se obtenían retenciones notablemente inferiores, siendo la máxima capacidad de retención 16 mg selenio g^{-1} (Tabla 5).

Tabla 4. Retención de arsénico en CTP en una atmósfera de gasificación a elevada temperatura.
Table 4. Retention of arsenic in CTP in a coal gasification atmosphere at high temperatures.

Temperatura (ºC)	Gasificación I		Gasificación II	
	CRM (mg g^{-1})	Eficiencia (%)	CRM (mg g^{-1})	Eficiencia (%)
350	1.49±0.14	19	2.37±0.32	16
550	15.9±0.62	100	17.0±2.98	73
750	24.1±3.34	99	2.04±0.04	---

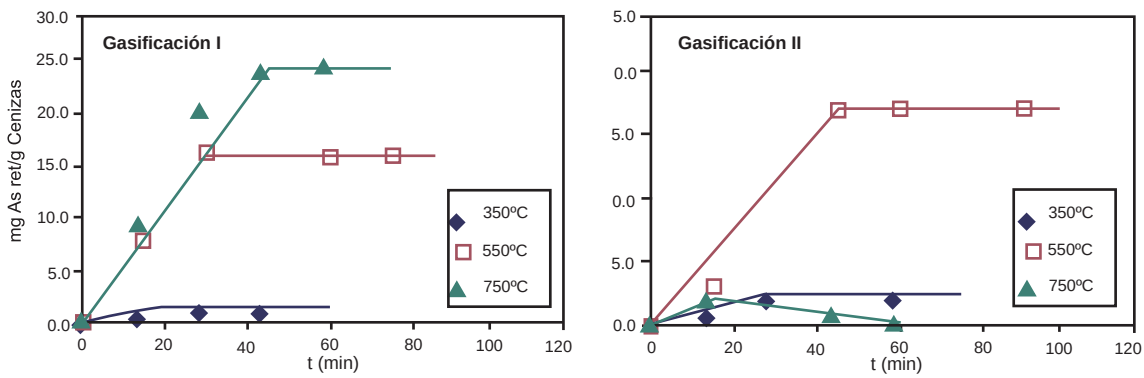

Figure 4. Retención de arsénico 4 en CTP en atmósfera de gasificación a alta temperatura.
Figure 4. Retention of arsenic in CTP in coal gasification atmosphere at high temperature.

Al igual que sucedía para el arsénico, la velocidad de retención se mantiene prácticamente constante hasta que se alcanza el límite en el cual no se adsorbe más selenio (Figura 5). La velocidad de la depende tanto de la temperatura como de la atmósfera de trabajo, siendo mayor en aquellos casos en los que se producen las mayores eficiencias.

Aunque no podemos descartar una posible contribución de un mecanismo de adsorción física en las cenizas, y a pesar de que la formación de nuevas especies no ha podido ser directamente identificadas mediante la caracterización de las muestras post-retención, los resultados obtenidos apoyarían la hipótesis de que en las cenizas volantes, al igual que en loa casos anteriores, tuvieran lugar retenciones de selenio debidas a reacciones químicas, tanto con el calcio presente en las cenizas como con el hierro también presente como óxido [9-10].

4. Conclusiones

La interacción de las especies gaseosas de arsénico y selenio tanto en atmósfera de combustión como de gasificación a baja y alta temperatura se produce fundamentalmente a través de reacciones químicas donde la materia mineral y concretamente elementos como el calcio y el hierro juegan un papel muy importante.

5. Agradecimientos

Este trabajo fue financiado por la Comunidad Europea (ECSC Proyectos 7220-ED/069 y 722-ED/095).

6. Referencias

[1]Diario Oficial de las comunidades Europeas. Decisión del Consejo de 4 de abril de 2001 relativa a la aprobación del Protocolo al Convenio de 1979 sobre contaminación atmosférica transfronteriza a gran distancia en materia de metales pesados L 134, 17.05.2001.

[2]Senior CL, Bool III LE, Srinivasachar S, Pease BR, Porle K. Pilot scale study of trace element vaporization and condensation during combustion of a pulverized sub-bituminous coal. Fuel Process Technol 2000; 63:149-165.

[3]Clarke LB. The fate of trace elements during coal combustion and gasification: an overview. Fuel 1993; 72:731-736.

[4]Clarke LB, Sloss LL. Trace elements-emissions from coal combustion and gasification, IEA Coal Research.1992, IEACR/49 111pp, London, 1992.

[5]López-Antón MA, Tascón JMD, Martínez-Tarazona MR. Retention of mercury in activated carbons in coal combustion and gasification flue gases. Fuel Process Technol 2002; 77-78:353-358.

[6]Bolt N, Van den Broeke WF, Enoch GD, Lefer JB. Slag utilization, hot gas clean up and waste water treatment research Coal and Power technology'90, Amsterdam, Netherlands, 21-23 May 1990.

[7]Brushell AJ, Willianmson J. The fate of trace elements in coal during gasification. Coal Science 8th International Conference on Coal Science, Oviedo, Spain, 10-15 Sep 1995, Amsterdam, the Netherlands, Elsevier Science B.V., vol2, 1967-1970, 1995.

[8]Andren AW, Klein DH, Talmi Y. Selenium in coal-fired steam plant emissions. Environ Sci Technol 1975; 9:856-858.

[9]European coal combustion products association e.V; http://www.ecoba.com

[10]Kalyoncu RS. Coal Combustion Products U.S. Geological Survey Minerals Yearbook-2000.

[11]Hasselriis F, Licata A. Analysis of heavy metal emission data from municipal waste combustion. J Hazard Mater 1996; 47:77-102.

[12]Díaz-Somoano M, López-Antón MA, Martínez-Tarazona MR. Determination of selenium by HG-ICP-MS in coal, fly ashes and sorbents used for flue gas cleaning. Fuel 2004; 83:231-235.

[13]López-Antón MA, Díaz-Somoano M, Spears DA, Martínez-Tarazona MR. Arsenic and selenium capture by fly ashes at low temperature. Environ Sci Technol 2006; 40:3947-3951.

Tabla 5. Retención de selenio en CTP en una atmósfera de gasificación a elevada temperatura.
Table 5. Retention of selenium in CTP in a coal gasification atmosphere at high temperature.

Temperatura (ºC)	Gasificación I		Gasificación II	
	CRM (mg g^{-1})	Eficiencia (%)	CRM (mg g^{-1})	Eficiencia (%)
550	25.5±3.32	50	16.1±1.64	33
750	25.4±2.66	83	24.5±3.01	67

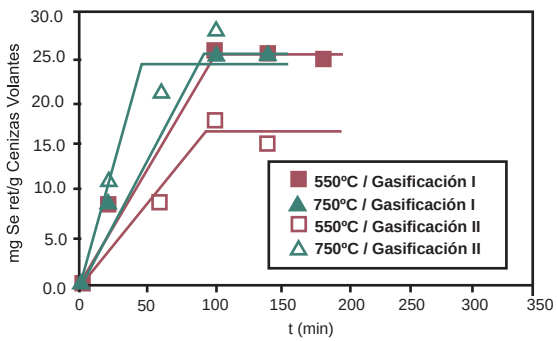

Figure 5. Retención de selenio en CTP en atmósfera de gasificación a alta temperatura.
Figure 5. Retention of selenium in CTP in coal gasification atmosphere at high temperature.

Thesis Review. Structure and properties of carbon nanofibers. Application as electrocatalyst support

S. del Río
Presented in 2011, ICB-CSIC
Supervisors: Rafael Moliner Álvarez and Mª Jesús Lázaro Elorri.ICB-CISIC. Miguel Luesma Castán 4, 50015 Zaragoza, Spain

1. Objectives and novelty

Novel carbon nanostructures have attracted a great interest as they combine unique properties that are difficult to be found in other conventional materials and, consequently, present the potential to fulfill the requirements of certain applications in fields of social and/or technological concerns like energy, catalysis, and electronics. Among them, carbon nanofibers (CNFs) are filaments of nanometer size (diameter up to 100 nm) formed by stacking graphene layers at a certain orientation. Their external porous structure together with their graphitic character that results in a high conductivity, make CNFs a promising candidate for their application in electrocatalytic systems. Carbon nanofibers are grown in a whisker-like mode by the precipitation of carbon on specific metal surfaces, so the shape of the metal particles and the diffusivity of carbon through them, determine the rate of growth, the orientation of the graphene layers and the size of the filament.

The present work aimed to gain an insight into the physical-chemical properties of carbon nanofibers and the relationship between those properties and the electrocatalytic behavior when used as catalyst support for their application in fuel cells. Several strategies are studied to modify CNFs properties: variation of synthesis operating conditions (temperature, gas composition and gas space velocity), functionalization with strong acids and chemical activation. A particularly interesting analysis of the electronic conductivity of CNFs is carried out for the first time, as this property can result of interest for several purposes (electronics, composites, etc.).

Afterwards, electrocatalysts are synthesized using CNFs as support to deposit nanoparticulated platinum and platinum-ruthenium alloys. These electrocatalysts are tested for the oxidation of methanol and ethanol as well as for the reduction of oxygen, which are the rate determining reactions in polymeric fuel cells. The study enables to select the most appropriate support material in terms of performance and durability, resulting in enhanced behavior with respect to the state of the art commercial supports.

2. Results

Carbon nanofibers, obtained by the catalytic decomposition of methane on a nickel-based catalyst, were observed to present different properties as a function of synthesis conditions (temperature, gas composition and space velocity), where temperature is remarkably the variable of highest influence. In general terms, textural properties like surface area and pore volume are favored by CNF synthesis at low temperature (550ºC) and high gas space velocity. On the contrary, the carbon ordering degree (crystallinity and low density of defects) and the related properties (e.g. electronic conductivity) are favored by the synthesis at relatively high temperatures (700-750 ºC) and introducing a certain concentration of hydrogen (10-15 %vol.). As an example, the SEM and HRTEM images of Figure 1 illustrate the morphological differences of CNFs obtained at two different synthesis temperatures.

CNF surface chemistry can be modified introducing oxygen groups by chemical oxidation with strong acids. Although carbonyl is the most abundant group,

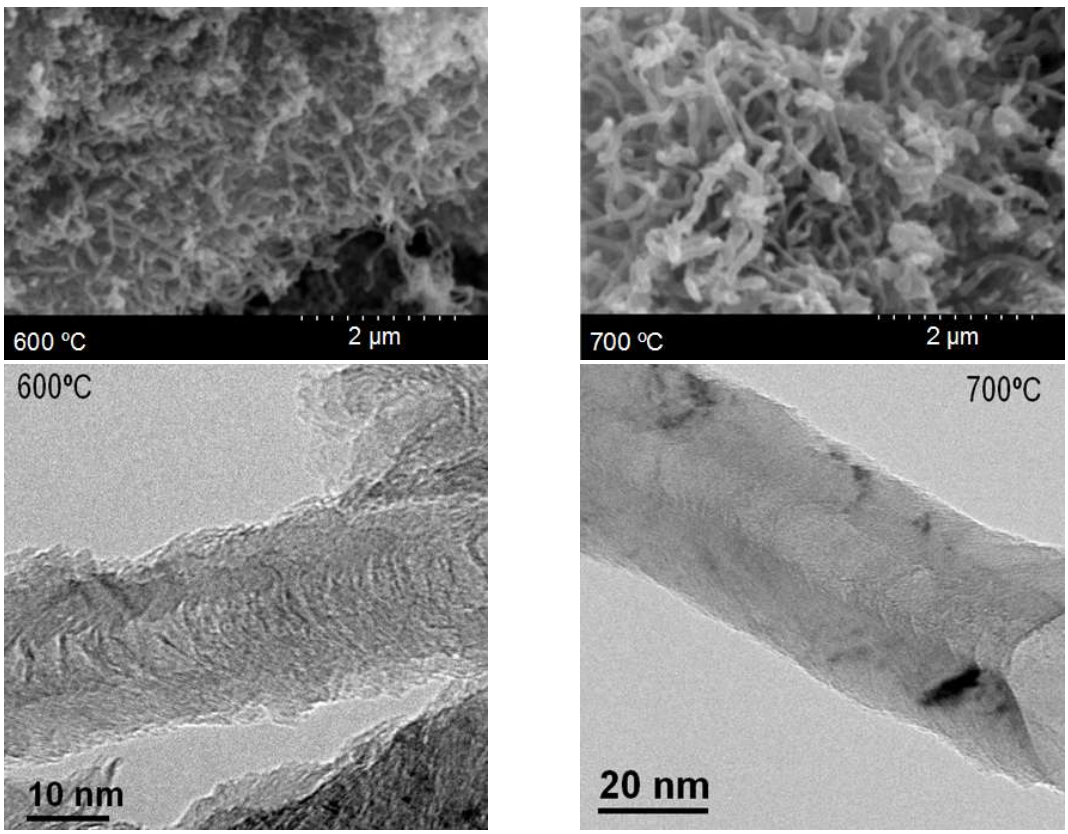

Figure 1. SEM (above) and HRTEM (below) images of carbon nanofibers obtained at 600ºC and 700ºC.

the relative amount of carboxylic acids and phenols can be increased by elevating oxidation temperature. Some properties are significantly changed with functionalization, such as the electronic conductivity, which decreases significantly with the introduction of oxygen. On the other hand, the activation of carbon nanofibers with potassium hydroxide is detrimental for their fibrous structure, increasing the surface area up to 60% by the fragmentation of the filaments.

Platinum and platinum-ruthenium nanoparticles were supported on CNFs by a microemulsion procedure (Figure 2). The main advantage of this method, compared to conventional impregnation, is the control of the metal crystal size (3 nm for Pt and 2 nm for PtRu alloys), with a narrow size distribution and independently of the support features, even for low surface area CNFs.

The electrocatalytic activity was found to depend on the carbon nanofibers characteristics. An optimum catalytic activity is obtained in a compromise situation between the properties derived from texture and those derived from crystallinity. High carbon crystalline order favors the catalyst specific activity (A/m^2_{metal}), whereas a high support surface area favors the dispersion of the nanoparticles, increasing the electrochemically active surface area (m^2/g_{metal}). The optimum mass activity (A/g_{metal}) is thus the product of these parameters and it is different for each electrochemical process. Methanol oxidation, this is, the anodic reaction of direct methanol fuel cells (DMFC), is favored using highly ordered carbon nanofibers. On the contrary, ethanol oxidation (anode of direct ethanol fuel cells) and oxygen reduction (cathodic reaction) are favored when supporting metal nanoparticles on CNF with improved textural properties. Higher performances were found for the Pt catalysts supported on CNF than supported on the state-of-the-art commercial carbon black (Vulcan), as can be seen in Figure 2.

Accelerated degradation tests were also carried out. The platinum sintering causes a decrease of the electrochemical surface area which causes a decrease in activity. In the case of carbon corrosion, it has been observed that carbon crystallinity favors the corrosion resistance. The best choice in terms of durability is again the result of a compromise situation between an appropriate dispersion of Pt nanoparticles (high surface area of CNFs), which prevents them from agglomeration, and a high crystallinity of the support, which reduces the corrosion rate.

3. Conclusions

The physical-chemical properties of CNFs as well as their surface chemistry can be tuned by an adequate choice of synthesis conditions, favoring a certain group of properties (porosity) or the other (crystallinity). Platinum-based catalysts have been supported on CNFs with different characteristics and their catalytic activity has been proven to depend on the support features, obtaining an optimum support for each electrochemical process in terms of performance and durability.

4. Related publications

[1] Lázaro MJ, Sebastián D, Suelves I, Moliner R, Carbon nanofiber growth optimization for their use as electrocatalyst support in proton exchange membrane (PEM) fuel cells. J Nanosci Nanotechnol, 2009; 9, 4353-4359.

[2] Sebastián D, Suelves I, Lázaro MJ, Moliner R, Carbon nanofibers as electrocatalyst support for fuel cells: the effect of hydrogen on their properties in CH4 decomposition. J Power Sources, 2009; 192, 51-56.

[3] Sebastián D, Calderón JC, González-Expósito JA, Pastor E, Martínez-Huerta MV, Suelves I, Moliner R, Lázaro MJ, Influence of carbon nanofiber properties as electrocatalyst support on the electrochemical performance for PEM fuel cells. Int J Hydrogen Energy, 2010; 35, 9934-9942.

[4] Sebastián D, Suelves I, Moliner R, Lázaro MJ, The effect of the functionalization of carbon nanofibers on their electronic conductivity. Carbon, 2010; 48, 4421-4431.

[5] Sebastián D, Lázaro MJ, Suelves I, Moliner R, Baglio V, Stassi A, Aricò AS, The influence of carbon nanofiber support properties on the oxygen reduction behavior in proton conducting electrolyte-based direct methanol fuel cells. Int J Hydrogen Energy, 2011; in press, doi:10.1016/j.ijhydene.2011.07.004.

[6] Sebastián D, Ruiz AG, Suelves I, Moliner R, Lázaro MJ, Baglio V, Stassi A, Aricò AS, Enhanced oxygen reduction activity and durability of Pt catalysts supported on carbon nanofibers. Appl Catal, B, 2012; 115-116, 269-275.

Full Thesis can be downloaded from the URL: http://digital.csic.es/handle/10261/37707

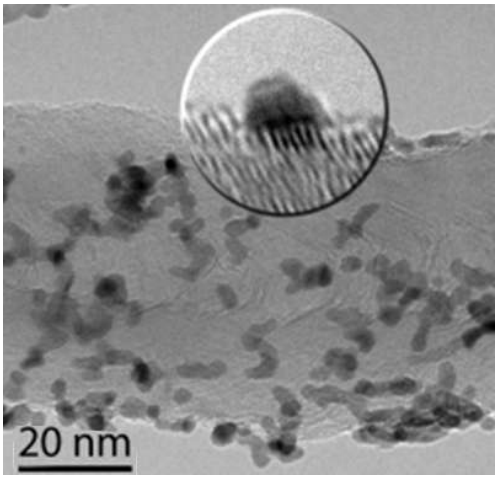

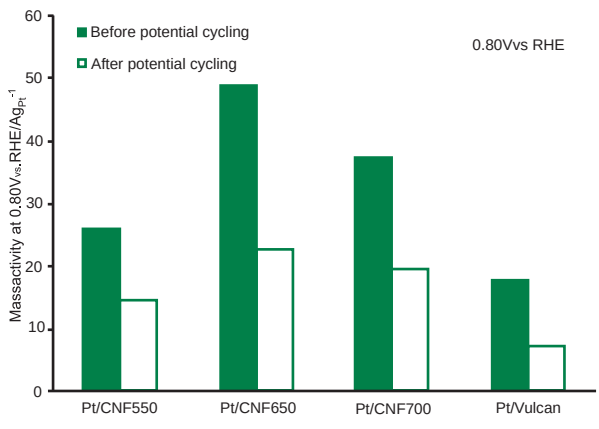

Figure 2. HRTEM image of Pt nanoparticles dispersed on CNFs (left); and oxygen reduction activity enhancement with the use of CNFs with respect to Vulcan commercial support (right).

Thesis Review. Electronic, mechanical and optical properties of atomically thin two-dimensional crystals

A. Castellanos-Gómez
Presented in 2011, Dpto. de Física Condensada. UAM, Madrid, Spain
Supervisors: Gabino Rubio-Bollinger and Nicolás Agraït (Universidad Autónoma de Madrid, Spain).

1. Objectives and novelty

The experimental realization of graphene, just a single atomic layer of graphite obtained by exfoliation, has triggered a revolution in the design of electronic devices and chemical sensors because of the unique electronic properties of graphene and its high sensitivity to the electrochemical environment. However, despite the interest aroused by this atomically thin crystal, just few groups have been able to study its local electronic properties by scanning probe microscopies. The reason is that these experiments require the development of non-standard procedures and protocols for producing, identifying and contacting electrically these crystals and specific scanning probe microscopy instrumentation.

The work carried out during this thesis has initiated a research line in the Low Temperature Laboratory of the Universidad Autónoma de Madrid, devoted to the study of electronic and mechanical properties of crystalline atomically thin two-dimensional sheets, such as graphene, MoS_2, $NbSe_2$ and mica by scanning probe microscopy.

2. Results

Development of new experimental tools:

This thesis describes the implementation of a combined scanning tunnelling microscope/atomic force microscope (STM/AFM) [1-3] developed to make possible the study of the local electronic properties of graphene. This combined microscope relies on an STM which has been supplemented with a force sensor based on a piezoelectric tuning fork [4] supplemented with recently developed carbon fibre tips [5] which optimize the performance of combined STM/AFM microscopes. The remarkable electrical and mechanical properties of carbon fibre make these tips more suitable for combined and/or simultaneous STM and AFM than conventional metallic tips. We have also demonstrated the suitability of these carbon-based tips as contact electrodes to form molecular junctions [6].

Ultraclean fabrication of graphene, graphene nanoribbons and other 2D materials:

We demonstrate that mechanical exfoliation can be employed to prepare atomically crystalline sheets as thin as just one-layer graphene, MoS_2, $NbSe_2$ and muscovite mica [7,8]. However, in our procedure the adhesive tape, commonly used in the mechanical exfoliation of graphene, has been substituted by a viscoelastic stamp, similar to the ones used in soft-lithography, thereby preventing the contamination of the atomically thin crystals with the adhesive.

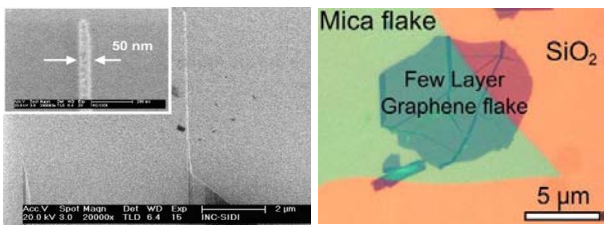

Figure 1. (left) Scanning electron micrograph of a 50 nm wide and 6 µm long graphene nanoribbon protruding from a multilayered graphene flake with both edges straight and parallel. (right) Optical micrograph of a few-layers graphene flake (< 10 layers) transferred onto an ultrathin mica flake (12 layes).

Interestingly, we found that this fabrication also produces graphene nanoribbons with lengths up to several tens of microns and widths in the range of 20 nm – 200 nm [9]. As these graphene nanoribbons occur spontaneously during the exfoliation procedure, it is expected that their edges follow one of the crystalline directions of the graphene lattice which would explain the remarkably straight edges of these exfoliated graphene nanoribbons.

Optical properties of 2D crystals:

We have developed a technique to determine the refractive index of atomically thin crystals based on the combination of quantitative optical microscopy and AFM [7,8]. The refractive index, both real and imaginary part, of these atomically thin sheets in the visible spectrum has been determined from a fit of the measured optical contrast to a Fresnel law based model. We have also obtained the optimal conditions of illumination wavelength and silicon oxide thickness to identify these crystals by means of optical microscopy.

Mechanical properties of a semiconducting analogue to graphene: the MoS_2

The mechanical properties of atomically thin membranes of MoS_2 have been probed by a bending test experiment carried out with an AFM [10]. From the analysis of the deformation *vs.* load characteristics curve of several tens of nanomembranes one can conclude that they are extremely flexible (deflections up to several tens of nanometers are reversible) and stiff (Young's modulus 0.30 ± 0.07 TPa). Indeed, their stiffness is comparable to that of one of the stiffest materials on Earth, graphene. This combination of mechanical properties makes these atomically thin MoS2 crystals excellent candidates for applications in flexible semiconductor devices.

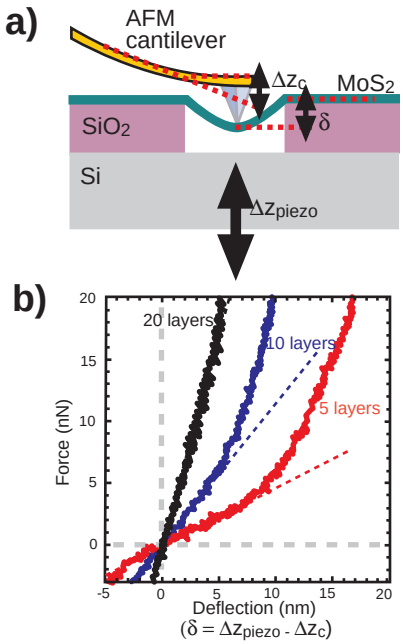

Figure 2. (a) Schematic diagram of the nanoscopic bending test experiment carried out on a freely suspended MoS_2 nanosheet. (b) Force vs. deflection traces measured at the center of the suspended part of MoS_2 nanosheets with 5, 10 and 20 layers in thickness.

Local electronic inhomogeneities in graphene

Finally, we have developed a combined STM/AFM microscopy technique to determine, with nanometer resolution, the spatial distribution of the electronic properties of graphene [11]. To spatially resolve the effect of the charged impurities on the electronic properties of graphene we have used the combined STM/AFM, developed in the first part of this thesis, to measure the topography of graphene and concomitantly a map of the local tunnelling barrier height. It has been found that the local tunnelling barrier height is very sensitive to the surface charge inhomogeneity of the graphene sheet induced by the presence of charged impurities in the substrate underneath.

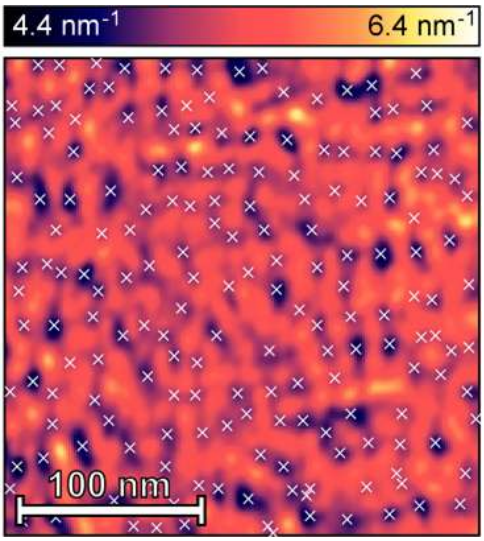

Figure 3. Spatial variation of the tunneling current decay constant on graphene measured in dynamic STM mode with our STM/AFM microscope. The image shows strong localized inhomogeneities (marked with white crosses) caused by the local modification of the tunneling barrier due to the presence of individual subsurface charges.

The local tunnelling barrier height maps showed localized inhomogeneities with 5 nm in radius, separated each other by about 20 nm, caused by the band bending induced by the presence of charged impurities in the substrate. From direct counting and statistical analysis of the spatial fluctuations of the tunnelling barrier height it was possible to determine, even at room conditions, the sign and the surface density of the charged impurities. The inhomogeneities do not show long range ordering and their sign and surface density obtained from the statistical analysis is consistent with the values obtained by macroscopic charge density measurements.

3. Conclusions

A combined effort on the development of new experimental tools and fabrication/characterization techniques has made possible to study the electronic, mechanical and optical properties of a new family of two-dimensional atomically thin crystals led by graphene.

In summary, novel procedures have been developed to produce and identify two-dimensional crystals of very diverse materials such as graphene, MoS_2, $NbSe_2$ and mica. In order to explore the local electronic properties of graphene, we have implemented a combined scanning tunnelling microscope / atomic force microscope, optimized to study small conductive nanocrystals deposited on insulating surfaces. This new tool has been employed to probe the spatial variations of the electronic properties of graphene on SiO_2 finding that the presence of charged impurities in the substrate induces localized inhomogeneities in the electronic properties of graphene.

4. Related publications

[1]Castellanos-Gomez, A.; Agraït, N.; Rubio-Bollinger, G. Dynamics of quartz tuning fork force sensors used in scanning probe microscopy. Nanotechnology 2009; 20(21): 215502.

[2]Castellanos-Gomez, A.; Agraït, N.; Rubio-Bollinger, G. Force-gradient-induced mechanical dissipation of quartz tuning fork force sensors used in atomic force microscopy. Ultramicroscopy 2011; 111(3): 186-190.

[3]Castellanos-Gomez, A., Agraït N., Rubio-Bollinger, G. Characterization and Optimization of Quartz Tuning Fork Based Force Sensors for Combined STM/AFM. In: H. Fuchs, H. Hosaka and B. Bushan. Ed. Springer-Verlag. 2012 (in press).

[4]Castellanos-Gomez, A.; Arroyo, C. R.; Agraït, N.; Rubio-Bollinger, G. Calibration of Piezoelectric Positioning Actuators Using a Reference Voltage-to-Displacement Transducer Based on Quartz Tuning Forks. Microscopy and Microanalysis 2012; (in press).

[5]Castellanos-Gomez, A.; Agraït, N.; Rubio-Bollinger, G. Carbon fibre tips for scanning probe microscopy based on quartz tuning fork force sensors. Nanotechnology 2010; 21(14): 145702.

[6]Castellanos-Gomez, A.; Bilan, S.; Zotti, L. a.; Arroyo, C. R.; Agraï¨t, N.; Carlos Cuevas, J.; Rubio-Bollinger, G. Carbon tips as electrodes for single-molecule junctions. Applied Physics Letters 2011; 99(12): 123105.

[7]Castellanos-Gomez, A.; Agraï¨t, N.; Rubio-Bollinger, G. Optical identification of atomically thin dichalcogenide crystals. Applied Physics Letters 2010, 96(21): 213116.

[8]Castellanos-Gomez, A.; Wojtaszek, M.; Tombros, N.; Agrait, N.; van Wees, B. J.; Rubio-Bollinger, G. Atomically thin mica flakes and their application as ultrathin insulating substrates for graphene. Small 2011; 7(17): 2491-2497.

[9]Moreno-Moreno, M.; Castellanos-Gomez, A.; Rubio-Bollinger, G.; Gomez-Herrero, J.; Agraït, N. Ultralong natural graphene nanoribbons and their electrical conductivity. Small 2009; 5(8): 924-927.

[10]Castellanos-Gomez, A.; Poot, M.; Steele, G. A.; van der Zant, H. S. J.; Agraït, N.; Rubio-Bollinger, G. Elastic Properties of Freely Suspended MoS2 Nanosheets. Advanced Materials 2012; 24(6): 772-5.

[11]Castellanos-Gomez, A.; Smit, R. H. M.; Agraït, N.; Rubio-Bollinger, G. Spatially resolved electronic inhomogeneities of graphene due to subsurface charges. Carbon 2012; 50(3): 932-938.

Full Thesis can be downloaded from:
http://www.tesisenred.net/handle/10803/49325